

Bounds on eigenstate thermalization

Shoki Sugimoto,^{1,*} Ryusuke Hamazaki,^{1,2} and Masahito Ueda^{3,4}

¹*Nonequilibrium Quantum Statistical Mechanics RIKEN Hakubi Research Team, RIKEN Cluster for Pioneering Research (CPR), Wako, Saitama 351-0198, Japan*

²*RIKEN iTHEMS, Wako, Saitama 351-0198, Japan*

³*Department of Physics, The University of Tokyo, 7-3-1 Hongo, Bunkyo-ku, Tokyo 113-0033, Japan*

⁴*RIKEN Center for Emergent Matter Science (CEMS), Wako 351-0198, Japan*

The eigenstate thermalization hypothesis (ETH), which asserts that every eigenstate of a many-body quantum system is indistinguishable from a thermal ensemble, plays a pivotal role in understanding thermalization of isolated quantum systems. Yet, no evidence has been obtained as to whether the ETH holds for *any* few-body operators in a chaotic system; such few-body operators include crucial quantities in statistical mechanics, such as the total magnetization, the momentum distribution, and their low-order thermal and quantum fluctuations. Here, we show the existence of upper and lower bounds on m_* such that *all* m -body operators with $m < m_*$ satisfy the ETH. For N -particle systems, these bounds are given in the form $\alpha_L \leq m_*/N \leq \alpha_U$, where α_L and α_U are N -independent positive numbers. We rigorously prove this statement for systems with Haar-distributed energy eigenstates and provide numerical evidence for generic systems with local and few-body interactions. Our results imply that generic systems satisfy the ETH for *any* few-body operators, including their thermal and quantum fluctuations.

Recent experiments in cold atoms and ions have demonstrated that quantum systems thermalize unitarily without heat reservoirs [1–8]. This finding brings up a striking possibility of incorporating statistical mechanics into a single framework of quantum mechanics – a scenario first envisioned by von Neumann about a century ago [9]. It has been argued that a single pure quantum state becomes indistinguishable from a thermal ensemble as far as few-body observables are concerned [10–18] due to the interplay between quantum entanglement and physical constraints on observable quantities such as locality or few-bodiness [10, 11, 14–18]. Depending on the choice of operators used to distinguish between a quantum state and a thermal ensemble, various notions of quantum-thermal equilibrium, such as microscopic thermal equilibrium (MITE) and macroscopic thermal equilibrium (MATE), have been introduced [10, 11, 13, 17, 19, 20].

The eigenstate thermalization hypothesis (ETH) [9, 21, 22] is widely believed to be the primary mechanism behind thermalization in isolated quantum systems. The ETH for an operator \hat{A} means that (i) every energy eigenstate of a system is in thermal equilibrium regarding the expectation value of \hat{A} and that (ii) off-diagonal elements of \hat{A} in an energy eigenbasis is vanishingly small. The ETH ensures thermalization of \hat{A} for any initial state with a macroscopically definite energy, barring massive degeneracy in the energy spectrum [14–18]. The ETH has been tested numerically for several local or few-body quantities [23–34]. However, whether the ETH holds for *all* few-body operators and whether it breaks down for many-body operators have yet to be fully addressed.

Von Neumann [9] and Reimann [35] proved the ETH for *almost all* Hermitian operators. However, their results do not imply that the ETH holds true for physically

realistic operators because *almost all* operators considered in Refs. [9, 35] involve highly nonlocal correlations that are close to N -body [36] and therefore unphysical. Some works [17, 37, 38] tested the ETH against several classes of few-body operators, such as local operators of a subsystem; however, their method cannot deal with generic few-body operators that act on an entire system, such as the total magnetization, the momentum distribution, and their thermal and quantum fluctuations.

In this Article, we show the existence of upper and lower bounds on m_* such that *all* m -body operators with $m < m_*$ satisfy the ETH. For N -particle systems with Haar-distributed energy eigenstates in arbitrary spatial dimensions, we prove that there exist N -independent constants α_L and α_U such that $\alpha_L \leq m_*/N \leq \alpha_U$ holds. Here, α_L and α_U depend only on the spin quantum number for spin systems or the particle-number density for Bose and Fermi systems (Figure 1). We also provide numerical evidence of the existence of the bound α_L for each of generic spin, Bose, and Fermi systems with local and few-body interactions (Figure 2). Our result is directly applicable to *any* few-body operators of interest in statistical mechanics and their thermal and quantum fluctuations without approximations, such as coarse-graining. In particular, our result implies that the ETH holds true even if we observe *any* low-order fluctuations of *arbitrary* few-body operators.

Our method also provides a quantitative criterion for deciding whether or not energy eigenstates of a system can be considered fully chaotic regarding the observables under consideration. This criterion is useful for systems with non-negligible finite-size effects, including ion and cold-atom systems, for which the thermodynamic limit cannot be taken [1–6, 39, 40].

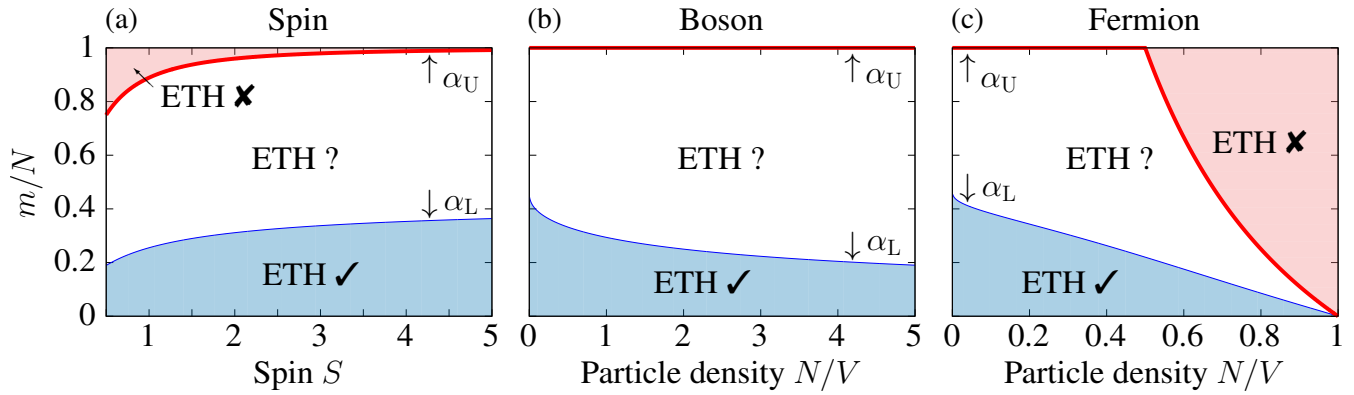


FIG. 1. **Regions of m/N where the ETH typically holds and breaks down for systems with Haar-distributed energy eigenstates.** The blue region (marked with “✓”) shows where the ETH typically holds for *all* operators in the space $\mathcal{A}^{[0,m]}$ of m -body operators. This region is delimited by α_L , which is defined as the largest value of α ($:= m/N$) such that $\dim \mathcal{A}_N^{[0,\alpha N]}/D \rightarrow 0$ in the thermodynamic limit for all $\alpha < \alpha_L$. The red region (marked with “✗”) shows where an ETH-breaking operator typically exists. This region is delimited by α_U , which is defined as the smallest value of α such that $\dim \mathcal{A}_N^{[0,\alpha N]}/D^2$ converges to a nonzero constant in the thermodynamic limit for all $\alpha > \alpha_U$. The integer m_* such that the ETH holds for *all* m -body operators with $m < m_*$ lies somewhere in the white region (marked with “?”).

Unified measure for quantum-thermal equilibrium.— While several measures and criteria of quantum-thermal equilibrium have been introduced in the literature [13, 17, 19, 20], they cannot be applied to generic few-body operators because they are defined for specific choices of operators, such as those acting only on a subsystem.

To quantitatively study how the ETH depends on physical constraints on observables, we introduce the following measure of the closeness to a thermal ensemble, which is applicable to an arbitrary set \mathcal{A} of observable quantities.

Definition 1 (Unified measure of quantum-thermal equilibrium). *To quantify the distance $\|\hat{\sigma} - \hat{\rho}_{\text{th}}\|$ between a quantum state $\hat{\sigma}$ and a thermal state $\hat{\rho}_{\text{th}}$, we introduce the following (semi-)norm,*

$$\|\hat{X}\|_p^{(\mathcal{A})} := \sup_{\substack{\hat{A} \in \mathcal{A} + \mathbb{R}\hat{I} \\ \hat{A} \neq 0}} \left| \text{tr} \left(\frac{\hat{A}^\dagger}{\|\hat{A}\|_q} \hat{X} \right) \right|, \quad (1)$$

where $p^{-1} + q^{-1} = 1$ with $(p, q) = (1, \infty)$ or $(2, 2)$, \mathbb{R} denotes the field of real numbers, and \hat{I} is the identity operator. Here, $\|\hat{A}\|_2$ is the Hilbert-Schmidt norm, and $\|\hat{A}\|_\infty$ is the operator norm. The operator \hat{X} is arbitrary and not necessarily Hermitian. Then, the (pseudo-)distance $\|\hat{\sigma} - \hat{\rho}_{\text{th}}\|_1^{(\mathcal{A})}$ with $\hat{\rho}_{\text{th}}$ being a thermal ensemble serves as a unified measure of quantum-thermal equilibrium.

For general \mathcal{A} , it is difficult or even impossible to calculate the supremum in $\|\cdot\|_1^{(\mathcal{A})}$, both numerically and analytically. However, we can bound $\|\cdot\|_1^{(\mathcal{A})}$ as $\|\cdot\|_1^{(\mathcal{A})} \leq \|\cdot\|_2^{(\mathcal{A})} \leq D^{1/2} \|\cdot\|_2^{(\mathcal{A})}$, where $\|\cdot\|_2^{(\mathcal{A})}$ is computable given an orthonormal basis of $\mathcal{A} + \mathbb{R}\hat{I}$ (see Methods). Among

$\|\cdot\|_p^{(\mathcal{A})}$ with $p \geq 1$, only $\|\cdot\|_1^{(\mathcal{A})}$ can be used to define a measure of quantum-thermal equilibrium because it is (i) invariant under a linear transformation: $\hat{A} \mapsto a'\hat{A} + b'$, (ii) dimensionless, and (iii) thermodynamically intensive [33], meaning that $\langle \hat{A} \rangle^{(\text{mc})}(E) / \|\hat{A}\|_q$ converges to a finite value in the thermodynamic limit. Here, $\langle \hat{A} \rangle^{(\text{mc})}(E)$ denotes the microcanonical average at energy E . The others, $\|\cdot\|_p^{(\mathcal{A})}$ with $p > 1$, are not suitable because they are not thermodynamically intensive (see Supplementary Information I).

We say that a quantum state $\hat{\sigma}$ is in thermal equilibrium relative to \mathcal{A} if $\|\hat{\sigma} - \hat{\rho}_{\text{th}}\|_1^{(\mathcal{A})} < \epsilon$ holds for a sufficiently small $\epsilon (> 0)$. This definition follows Refs. [19, 20]; however, we here concern only the expectation value of $\hat{A} \in \mathcal{A}$ and not the probability distribution over the spectrum of \hat{A} . Nonetheless, our framework can deal with the probability distribution by including sufficiently high powers of \hat{A} in \mathcal{A} , offering finer control over the precision in observing the distribution of \hat{A} . By appropriately choosing \mathcal{A} , our notion of quantum-thermal equilibrium unifies previously introduced ones, such as subsystem thermal equilibrium [10, 11, 37, 38], microscopic thermal equilibrium (MITE), and macroscopic thermal equilibrium (MATE) [17, 19, 20] (see Supplementary Information II).

Many of the previous works that numerically tested the ETH with respect to several operators $\hat{A}_1, \dots, \hat{A}_J$ [23–32] essentially set $\mathcal{A} = \{\hat{A}_1, \dots, \hat{A}_J\}$. However, if one really wants to distinguish an energy eigenstate from $\hat{\rho}_{\text{th}}$ without any exception, one should use not only a limited number of quantities but *all* the quantities compatible with physical constraints under consideration.

Measure of the ETH.— To introduce the measure of the ETH, which requires (i) *all* energy eigenstates to be in thermal equilibrium and (ii) *all* off-diagonal elements of an observable in an energy eigenbasis are vanishingly small, we introduce

$$\Lambda_p^{(\hat{H}, \mathcal{A})}(E) := \max_{|E_\alpha\rangle, |E_\beta\rangle \in \mathcal{H}_{E, \Delta E}} \left\| \hat{\rho}_{\alpha\beta} - \hat{\rho}_{\delta E}^{(\text{mc})}(E_\alpha) \delta_{\alpha\beta} \right\|_p^{(\mathcal{A})},$$

where $p = 1$ or 2 , $\hat{\rho}_{\alpha\beta} := |E_\alpha\rangle\langle E_\beta|$ with $|E_\alpha\rangle$ being an energy eigenstate with eigenenergy E_α , and $\hat{\rho}_{\delta E}^{(\text{mc})}(E_\alpha)$ is the microcanonical ensemble within the energy shell $\mathcal{H}_{E_\alpha, \delta E} := \text{span}\{|E_\gamma\rangle \mid |E_\gamma - E_\alpha| < \delta E\}$. As is the case for the norm $\|\cdot\|_p^{(\mathcal{A})}$, $\Lambda_1^{(\hat{H}, \mathcal{A})}$ is a proper measure of the ETH, and $\Lambda_2^{(\hat{H}, \mathcal{A})}$ will be used to bound $\Lambda_1^{(\hat{H}, \mathcal{A})}$. The ETH holds for *all* operators in \mathcal{A} if and only if $\lim_{N \rightarrow \infty} \Lambda_1^{(\hat{H}, \mathcal{A})} = 0$. Indeed, if $\Lambda_1^{(\hat{H}, \mathcal{A})}$ is sufficiently small, *all* the operators in \mathcal{A} give almost the same expectation values for $|E_\alpha\rangle$ and $\hat{\rho}_{\delta E}^{(\text{mc})}(E_\alpha)$, and their off-diagonal elements within the energy shell $\mathcal{H}_{E_\alpha, \delta E}$ become sufficiently small. In that sense, $\Lambda_1^{(\hat{H}, \mathcal{A})}$ is the most sensitive ETH measure ever. If $\Lambda_1^{(\hat{H}, \mathcal{A})}$ remains finite in the limit $N \rightarrow \infty$, there exists an operator $\hat{A} \in \mathcal{A}$ such that the expectation values of \hat{A} for $|E_\alpha\rangle$ and $\hat{\rho}_{\delta E}^{(\text{mc})}$ are different, or some off-diagonal elements of \hat{A} within $\mathcal{H}_{E_\alpha, \delta E}$ remain nonnegligible. Therefore, the ETH with respect to \mathcal{A} breaks down in this case.

Distribution of $\Lambda_1^{(\hat{H}, \mathcal{A})}(E)$ for systems with Haar-distributed energy eigenstates.— Having introduced the measure of the ETH and the bounds on $\|\cdot\|_1^{(\mathcal{A})}$ in terms of the computable quantity $\|\cdot\|_2^{(\mathcal{A})}$, we are in a position to discuss the validity of the ETH relative to a set of observables \mathcal{A} . For systems with Haar-distributed energy eigenstates, we can derive the following theorem.

Theorem 1. *Let \mathcal{G}_{inv} be an invariant random matrix ensemble, the eigenvectors of whose matrices are distributed according to the unitary Haar measure. We set $D := \dim \mathcal{H}$ and $M := \dim \mathcal{A}$. Then, for any D -independent $\epsilon > 0$, we have*

$$\frac{1}{8} \frac{M}{D^2} \leq (\Lambda_1^{(\hat{H}, \mathcal{A})})^2 + \mathcal{O}\left(\frac{D^\epsilon}{\sqrt{D}}\right) \leq \frac{M}{D} \quad (2)$$

and $M/(8D^2) \leq (\Lambda_2^{(\hat{H}, \mathcal{A})})^2 + \mathcal{O}(D^\epsilon/\sqrt{D}) \leq M/D^2$ for almost all $\hat{H} \in \mathcal{G}_{\text{inv}}$, whose fraction is bounded from below by $1 - \exp(-\mathcal{O}(D^{2\epsilon}))$.

Outline of the proof Theorem 1. The proof goes in three main steps. (i) First, we consider the square of the p -norm $\|\hat{\rho}_{\alpha\beta} - \hat{\rho}_{\delta E}^{(\text{mc})}(E_\alpha) \delta_{\alpha\beta}\|_p^{(\mathcal{A})}$ with $p = 1, 2$, which we denote by $f_p^{(\alpha\beta)}(\hat{U})$, and calculate the average of $f_2^{(\alpha\beta)}$ over the Haar measure as $\mathbb{E}[f_2^{(\alpha\beta)}] \simeq M/D^2$. (ii) Second, we show that $f_p^{(\alpha\beta)}(\hat{U})$ is Lipschitz continuous for

each index $(\alpha\beta)$ so that we can apply the concentration inequality of the Haar measure [41–43]. We also show that their Lipschitz constant is independent of both D and the index $(\alpha\beta)$. (iii) Finally, we apply the concentration inequality to $f_p^{(\alpha\beta)}(\hat{U})$ for each index $(\alpha\beta)$ such that $|E_\alpha\rangle, |E_\beta\rangle \in \mathcal{H}_{E, \Delta}$. Since the concentration inequality implies that the distribution of a Lipschitz function is sharply concentrated around its average, we can derive the inequality (2) from that for each $\mathbb{E}[f_1^{(\alpha\beta)}]$. See Methods for the complete proof. ■

With Theorem 1, we can test whether or not the ETH regarding \mathcal{A} typically holds in \mathcal{G}_{inv} by counting the dimension of the operator space \mathcal{A} . In the thermodynamic limit, the ETH regarding \mathcal{A} typically holds if the upper bound of Eq. (2) vanishes, and an ETH-breaking operator typically exists in \mathcal{A} if the lower bound of Eq. (2) converges to a finite value. The relation $(\Lambda_2^{(\hat{H}, \mathcal{A})})^2 \simeq M/D^2$ in Theorem 1 provides a quantitative criterion, applicable to finite-size systems, for deciding whether a realistic Hamiltonian \hat{H} can be considered to have fully chaotic eigenstates in terms of \mathcal{A} . The contraposition of Theorem 1 implies that if a given Hamiltonian violates $(\Lambda_2^{(\hat{H}, \mathcal{A})})^2 \simeq M/D^2$, then it is not typical in \mathcal{G}_{inv} . Since the Hamiltonians in \mathcal{G}_{inv} are statistically invariant under unitary transformations, typical Hamiltonians in \mathcal{G}_{inv} can be considered to have no structure. Hence, the existence of an operator $\hat{A} \in \mathcal{A}$ that violates $(\Lambda_2^{(\hat{H}, \mathcal{A})})^2 \simeq M/D^2$ implies that the eigenstate of \hat{H} has a “structure” that can be detected by \hat{A} . Furthermore, by comparing the N -dependence of $(\Lambda_2^{(\hat{H}, \mathcal{A})})^2$ for a realistic Hamiltonian \hat{H} with that of M/D^2 , we can infer the N -dependence of $\Lambda_1^{(\hat{H}, \mathcal{A})}$ for large N that is difficult to access.

Rigorous upper and lower bounds for the ETH.— We apply Theorem 1 to test the ETH for few- and many-body observables. For N -site spin- S systems, we define the m -body operator space $\mathcal{A}_N^{[0, m]}$ as the space of operators that can be expressed as a linear combination of operators acting nontrivially on at most m spins [36]. For Bose and Fermi systems, we define $\mathcal{A}_N^{[0, m]}$ to be the space of operators that can be written as a linear combination of products of m annihilation operators and m creation operators.

By counting the dimension of $\mathcal{A}_N^{[0, m]}$ and that of the total Hilbert space, we can apply Theorem 1 to obtain the following theorem.

Theorem 2 (Upper and lower bounds for the ETH). *Let m_* be the largest number such that the ETH with respect to $\mathcal{A}^{[0, m]}$ typically holds in \mathcal{G}_{inv} for all $m < m_*$. Then, there exist N -independent constants $\alpha_L^H \in (0, 1/2]$ and $\alpha_U^H > 0$ that satisfy $\alpha_L^H \leq m_*/N \leq \alpha_U^H$. Moreover, the ETH measure decays exponentially in the system size when $m/N < \alpha_L^H$.*

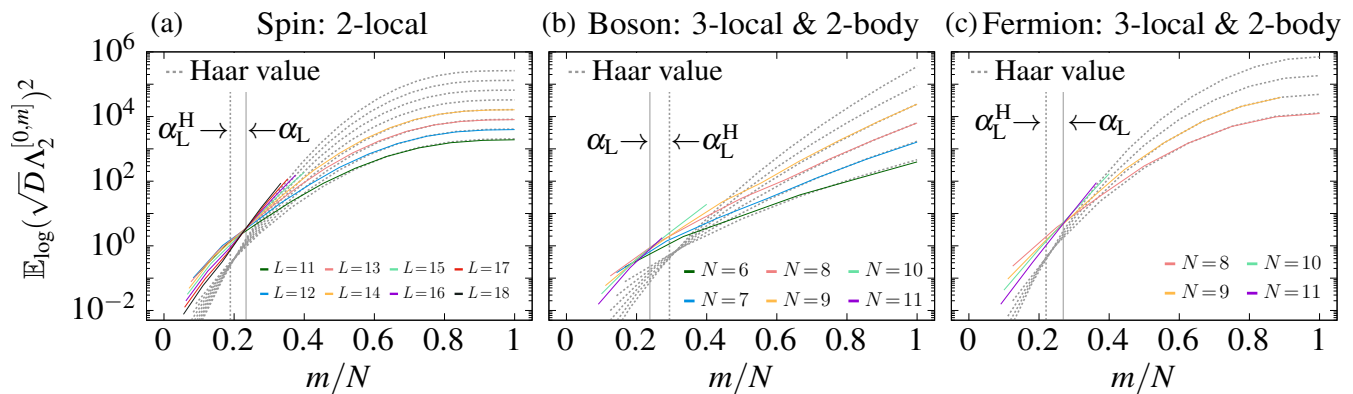


FIG. 2. **Ensemble average of the upper bound of the (diagonal) ETH measure for Hamiltonians with local and few-body interactions.** The quantity $\Lambda_2^{[0,m]}$ is calculated in the energy window centered at energy $E = (E_{\max} + E_{\min})$ with width $2\Delta = 0.05(E_{\max} - E_{\min})$, where E_{\max}/\min is the maximum/minimum of the energy spectrum. The symbol \mathbb{E}_{\log} denotes the geometric mean. The gray vertical solid lines indicate the points α_L and α_U where the maximum difference of the curves for different system sizes is minimized. The quantity α_L^H denotes the value of α_L for the Haar measure. The width of the microcanonical energy shell is set to $\delta E = 0.2(E_{\max} - E_{\min})/V$, which is sufficiently small for the system sizes of the numerical calculation (up to 18 spins for spin systems, and up to 11 particles for Bose and Fermi systems.) We consider three ensembles: (a) spin systems consisting of up to 2-local terms, i.e., nearest-neighbor interactions and on-site potentials; (b) Bose and (c) Fermi systems consisting of 3-local and 2-body terms, i.e., products of two creation and two annihilation operators acting on three consecutive sites. Different colors show data for different system sizes. There are points where curves for different system sizes almost intersect, which can clearly be observed for spin and Fermi systems. While it is less clear for Bose systems up to 11 particles, the intersections still occur in a narrow region around $m/N \sim 0.2$. On the left of the intersections, the upper bound of the ETH measure decreases as the system size increases, indicating that the ETH holds in this region for generic systems. These results verify the existence of the lower bound on the ratio m_*/N for generic Hamiltonians with local and few-body interactions, which is a part of Conjecture 1.

Outline of the proof Theorem 2. We define α_L^H as the largest value such that $\dim \mathcal{A}_N^{[0,\alpha N]}/D \rightarrow 0$ in the thermodynamic limit for all $\alpha < \alpha_L^H$ and α_U^H as the smallest value such that $\dim \mathcal{A}_N^{[0,\alpha N]}/D^2$ converges to a positive value in the thermodynamic limit for all $\alpha \geq \alpha_U^H$. Then, Theorem 1 gives $\alpha_L^H \leq m_*/N \leq \alpha_U^H$. Direct calculations for each of spin, Bose, and Fermi systems show $\alpha_L^H \in (0, 1/2]$ and the exponential decay of the ETH measure when $m/N < \alpha_L^H$ (see Methods for the complete proof). ■

The existence of an N -independent lower bound α_L on m_*/N implies that the ETH holds true even if we observe $\mathcal{O}(N)$ -body operators in systems with Haar-distributed energy eigenstates. Because our result is not restricted to the operators acting only on subsystems, we conclude that the decomposition of the total system into a subsystem and the rest is not essential for the ETH to hold. For the same reason, our result directly applies to any operators acting on the whole system, which cannot exactly be dealt with in previous works [17, 37]. These operators include extensive sums of local operators (e.g., total magnetization), few-body operators (e.g., momentum distributions), and low-order powers of these quantities. Since the central moments of a few-body operator \hat{A} are polynomials of \hat{A} and their values scale polynomially in N , the exponential decay of the ETH measure implies that *the ETH typically holds in \mathcal{G}_{inv} including any low-order*

fluctuations of any few-body operators.

Numerical tests for locally interacting systems.—

Theorems 1 and 2 are rigorous theorems that hold for Hamiltonians with Haar-distributed eigenstates. Ensembles of such Hamiltonians have been used to model chaotic quantum systems. In particular, the typicality of the ETH regarding several observables has been proved for (nonlocal) Hamiltonians with [9, 17, 35] and without [44–46] Haar-distributed eigenstates. Theorem 1 generalizes these lines of studies by considering arbitrary sets of test observables, and Theorem 2 illustrates a benefit of such a generalization. However, such Hamiltonians typically contain highly nonlocal and $\mathcal{O}(N)$ -body terms and sometimes lead to conclusions different from those in locally interacting systems. Indeed, a number of studies have revealed deviations from the Haar measure in chaotic quantum systems with local and few-body interactions [36, 47–50]. In addition, a typical unitary sampled from the Haar measure transforms local and few-body operators to highly nonlocal and $\mathcal{O}(N)$ -body ones. Therefore, properties of individual test operators, such as locality or few-body nature, do not play a fundamental role in Theorem 1, and only the dimension of the operator space appears in the inequality (2).

A highly nontrivial aspect of chaotic quantum systems is that some predictions of the Haar measure, including the ETH, turn out to be qualitatively correct in systems

with local and few-body interactions [23, 25, 29, 33, 34]. Therefore, we pose the following conjecture on the basis of Theorem 2 and numerically test it for Hamiltonians with local and few-body interactions:

Conjecture 1. *Let m_* be the largest number such that the ETH with respect to $\mathcal{A}^{[0,m]}$ holds for all $m < m_*$. For a generic nonintegrable system, there exist N -independent constants $\alpha_L \in (0, 1/2]$ and $\alpha_U > 0$ that satisfy $\alpha_L \leq m_*/N \leq \alpha_U$.*

We introduce ensembles of Hamiltonians with local and few-body interactions for each of spin, Bose, and Fermi systems. For spin systems, we introduce an ensemble of Hamiltonians consisting of 2-local terms, i.e., nearest-neighbor interactions and on-site potentials. For Bose and Fermi systems, we consider an ensemble of Hamiltonians consisting of 3-local and 2-body terms, i.e., terms involving two annihilation and two creation operators acting nontrivially on consecutive three sites. To facilitate calculations for large system sizes, we impose the translation and/or reflection symmetries on each Hamiltonian in the ensembles by projecting it onto the zero-momentum and even-parity sector (see Methods for the precise constructions).

Figure 2 shows the average of the upper bound of the ETH measure over those ensembles as a function of the ratio m/N . For spin and Fermi ensembles, we observe that there exists a value α_L of m/N where the curves for different system sizes nearly intersect. In the region with $m/N > \alpha_L$ and $m/N < \alpha_L$, the average of the upper bound increases and decreases as the system size increases, respectively. This implies that the ETH with respect to all m -body operators holds when $m/N < \alpha_L$, meaning that $\alpha_L \leq m_*/N$ for the spin and Fermi ensembles with local and few-body interactions. These results support Conjecture 1. For Bose systems, the curves for different system sizes do not intersect as sharply as spin and Fermi systems. Still, we observe that they nearly intersect in the region around $m/N \sim 0.2$. On the right side of the region, the average of the upper bound increases as the system size increases, and on the left side of the region, the average of the upper bound decreases as the system size increases. These behaviors also support Conjecture 1, and we expect that the intersection would become sharper if we could add data for larger system sizes beyond the currently accessible ones.

It is remarkable that our numerical results for systems with local and few-body interactions support Conjecture 1 despite that it can only be proved for systems with Haar-distributed energy eigenstates (Theorem 2), whose Hamiltonians typically consist of highly nonlocal and $\mathcal{O}(N)$ -body terms. The existence of a nontrivial upper bound on m_*/N is also numerically verified for spin systems (see Supplementary Information V). However, the numerical calculation of the $\Lambda_2^{(\hat{H}, \mathcal{A})}$ for large m is quite costly for Bose and Fermi systems, which prevents

the numerical verification of the existence of the upper bound on m_*/N for Bose and Fermi systems with currently available computational resources.

We also test Conjecture 1 for concrete nonintegrable systems where the ETH is numerically verified to hold, namely, the Ising model with transverse and longitudinal field [29], the Bose-Hubbard model at unit filling [25], and the spinless fermions with next-nearest-neighbor terms [24] at half filling. However, Conjecture 1 is neither validated nor invalidated for all of these concrete models. For these models, finite-size effects are significant that we cannot safely determine whether the upper bound of the ETH measure decreases for large system sizes even for $m = 1$ (see Supplementary Information VII). This fact suggests that the inequality $\|\cdot\|_1^{(\mathcal{A})} \leq \sqrt{D} \|\cdot\|_2^{(\mathcal{A})}$ is too loose to test Conjecture 1 for those concrete physical models. It remains to be an important future task to validate (or invalidate) Conjecture 1 for prototypical nonintegrable systems, e.g., by finding better bounds on the ETH measure.

-
- [1] S. Trotzky, Y.-A. A. Chen, A. Fleisch, I. P. McCulloch, U. Schollwöck, J. Eisert, and I. Bloch, Probing the relaxation towards equilibrium in an isolated strongly correlated one-dimensional Bose gas, *Nature Physics* **8**, 325 (2012).
 - [2] T. Langen, R. Geiger, M. Kuhnert, B. Rauer, and J. Schmiedmayer, Local emergence of thermal correlations in an isolated quantum many-body system, *Nature physics* **9**, 640 (2013).
 - [3] G. Clos, D. Porras, U. Warring, and T. Schaetz, Time-Resolved Observation of Thermalization in an Isolated Quantum System, *Physical Review Letters* **117**, 170401 (2016).
 - [4] A. M. Kaufman, M. E. Tai, A. Lukin, M. Rispoli, R. Schittko, P. M. Preiss, and M. Greiner, Quantum thermalization through entanglement in an isolated many-body system, *Science* **353**, 794 (2016).
 - [5] C. Neill, P. Roushan, M. Fang, Y. Chen, M. Kolodrubetz, Z. Chen, A. Megrant, R. Barends, B. Campbell, B. Chiaro, A. Dunsworth, E. Jeffrey, J. Kelly, J. Mutus, P. J. J. O'Malley, C. Quintana, D. Sank, A. Vainsencher, J. Wenner, T. C. White, A. Polkovnikov, and J. M. Martinis, Ergodic dynamics and thermalization in an isolated quantum system, *Nature Physics* **12**, 1037 (2016).
 - [6] Y. Tang, W. Kao, K.-Y. Li, S. Seo, K. Mallayya, M. Rigol, S. Gopalakrishnan, and B. L. Lev, Thermalization near Integrability in a Dipolar Quantum Newton's Cradle, *Physical Review X* **8**, 021030 (2018).
 - [7] A. P. Orioli, A. Signoles, H. Wildhagen, G. Günter, J. Berges, S. Whitlock, and M. Weidemüller, Relaxation of an Isolated Dipolar-Interacting Rydberg Quantum Spin System, *Physical Review Letters* **120**, 63601 (2018).
 - [8] T. Langen, R. Geiger, and J. Schmiedmayer, Ultracold Atoms Out of Equilibrium, *Annual Review of Condensed Matter Physics* **6**, 201 (2015).

- [9] J. von Neumann, Proof of the ergodic theorem and the H-theorem in quantum mechanics, *The European Physical Journal H* **35**, 201 (2010).
- [10] S. Popescu, A. J. Short, and A. Winter, Entanglement and the foundations of statistical mechanics, *Nature Physics* **2**, 754 (2006).
- [11] S. Goldstein, J. L. Lebowitz, R. Tumulka, and N. Zanghì, Canonical Typicality, *Physical Review Letters* **96**, 050403 (2006).
- [12] P. Reimann, Typicality for Generalized Microcanonical Ensembles, *Physical Review Letters* **99**, 160404 (2007).
- [13] H. Tasaki, Typicality of Thermal Equilibrium and Thermalization in Isolated Macroscopic Quantum Systems, *Journal of Statistical Physics* **163**, 937 (2016).
- [14] A. Polkovnikov, K. Sengupta, A. Silva, and M. Vengalattore, Colloquium: Nonequilibrium dynamics of closed interacting quantum systems, *Reviews of Modern Physics* **83**, 863 (2011).
- [15] L. D'Alessio, Y. Kafri, A. Polkovnikov, and M. Rigol, From quantum chaos and eigenstate thermalization to statistical mechanics and thermodynamics, *Advances in Physics* **65**, 239 (2016).
- [16] C. Gogolin and J. Eisert, Equilibration, thermalisation, and the emergence of statistical mechanics in closed quantum systems, *Reports on Progress in Physics* **79**, 056001 (2016).
- [17] T. Mori, T. N. Ikeda, E. Kaminishi, and M. Ueda, Thermalization and prethermalization in isolated quantum systems: a theoretical overview, *Journal of Physics B: Atomic, Molecular and Optical Physics* **51**, 112001 (2018).
- [18] J. M. Deutsch, Eigenstate thermalization hypothesis, *Reports on Progress in Physics* **81**, 082001 (2018).
- [19] S. Goldstein, D. A. Huse, J. L. Lebowitz, and R. Tumulka, Thermal Equilibrium of a Macroscopic Quantum System in a Pure State, *Physical Review Letters* **115**, 100402 (2015).
- [20] S. Goldstein, D. A. Huse, J. L. Lebowitz, and R. Tumulka, Macroscopic and microscopic thermal equilibrium, *Annalen der Physik* **529**, 1600301 (2017).
- [21] J. M. Deutsch, Quantum statistical mechanics in a closed system, *Physical Review A* **43**, 2046 (1991).
- [22] M. Srednicki, Chaos and quantum thermalization, *Physical Review E* **50**, 888 (1994).
- [23] M. Rigol, V. Dunjko, and M. Olshanii, Thermalization and its mechanism for generic isolated quantum systems, *Nature* **452**, 854 (2008).
- [24] M. Rigol, Quantum quenches and thermalization in one-dimensional fermionic systems, *Physical Review A* **80**, 053607 (2009).
- [25] G. Biroli, C. Kollath, and A. M. Läuchli, Effect of Rare Fluctuations on the Thermalization of Isolated Quantum Systems, *Physical Review Letters* **105**, 250401 (2010).
- [26] L. F. Santos and M. Rigol, Localization and the effects of symmetries in the thermalization properties of one-dimensional quantum systems, *Physical Review E* **82**, 031130 (2010).
- [27] R. Steinigeweg, J. Herbrych, and P. Prelovšek, Eigenstate thermalization within isolated spin-chain systems, *Physical Review E* **87**, 012118 (2013).
- [28] W. Beugeling, R. Moessner, and M. Haque, Finite-size scaling of eigenstate thermalization, *Physical Review E* **89**, 042112 (2014).
- [29] H. Kim, T. N. Ikeda, and D. A. Huse, Testing whether all eigenstates obey the eigenstate thermalization hypothesis, *Physical Review E* **90**, 052105 (2014).
- [30] R. Mondaini, K. R. Fratus, M. Srednicki, and M. Rigol, Eigenstate thermalization in the two-dimensional transverse field Ising model, *Physical Review E* **93**, 032104 (2016).
- [31] R. Mondaini and M. Rigol, Eigenstate thermalization in the two-dimensional transverse field Ising model. II. Off-diagonal matrix elements of observables, *Physical Review E* **96**, 012157 (2017).
- [32] D. Jansen, J. Stolpp, L. Vidmar, and F. Heidrich-Meisner, Eigenstate thermalization and quantum chaos in the Holstein polaron model, *Physical Review B* **99**, 155130 (2019).
- [33] S. Sugimoto, R. Hamazaki, and M. Ueda, Test of the Eigenstate Thermalization Hypothesis Based on Local Random Matrix Theory, *Physical Review Letters* **126**, 120602 (2021).
- [34] S. Sugimoto, R. Hamazaki, and M. Ueda, Eigenstate Thermalization in Long-Range Interacting Systems, *Physical Review Letters* **129**, 030602 (2022).
- [35] P. Reimann, Generalization of von Neumann's Approach to Thermalization, *Physical Review Letters* **115**, 010403 (2015).
- [36] R. Hamazaki and M. Ueda, Atypicality of Most Few-Body Observables, *Physical Review Letters* **120**, 080603 (2018).
- [37] J. R. Garrison and T. Grover, Does a Single Eigenstate Encode the Full Hamiltonian?, *Physical Review X* **8**, 021026 (2018).
- [38] A. Dymarsky, N. Lashkari, and H. Liu, Subsystem eigenstate thermalization hypothesis, *Physical Review E* **97**, 12140 (2018).
- [39] M. Gring, M. Kuhnert, T. Langen, T. Kitagawa, B. Rauer, M. Schreitl, I. Mazets, D. Adu Smith, E. Demler, J. Schmiedmayer, D. A. Smith, E. Demler, and J. Schmiedmayer, Relaxation and prethermalization in an isolated quantum system, *Science* **337**, 1318 (2012).
- [40] B. Neyenhuis, J. Zhang, P. W. Hess, J. Smith, A. C. Lee, P. Richerme, Z.-X. Gong, A. V. Gorshkov, and C. Monroe, Observation of prethermalization in long-range interacting spin chains, *Science Advances* **3**, e1700672 (2017).
- [41] M. Ledoux, *The concentration of measure phenomenon*, 89 (American Mathematical Society, 2001).
- [42] E. S. Meckes, *The Random Matrix Theory of the Classical Compact Groups* (Cambridge University Press, 2019) pp. 1–212.
- [43] A. A. Mele, Introduction to Haar Measure Tools in Quantum Information: A Beginner's Tutorial, *Quantum* **8**, 1340 (2024).
- [44] G. Cipolloni, L. Erdős, and D. Schröder, Eigenstate Thermalization Hypothesis for Wigner Matrices, *Communications in Mathematical Physics* **388**, 1005 (2021).
- [45] A. Adhikari, S. Dubova, C. Xu, and J. Yin, Eigenstate thermalization hypothesis for generalized Wigner matrices, *Electronic journal of probability* **29**, 1 (2024).
- [46] L. Erdős and V. Riabov, Eigenstate Thermalization Hypothesis for Wigner-type matrices, *Communications in mathematical physics* **405**, 282 (2024).
- [47] Y. Y. Atas and E. Bogomolny, Multifractality of eigenfunctions in spin chains, *Physical Review E* **86**, 021104 (2012).
- [48] A. Bäcker, M. Haque, and I. M. Khaymovich, Multifractal

- tal dimensions for random matrices, chaotic quantum maps, and many-body systems, [Physical Review E **100**, 032117 \(2019\)](#).
- [49] Y. Huang, Universal entanglement of mid-spectrum eigenstates of chaotic local Hamiltonians, [Nuclear physics. B **966**, 115373 \(2021\)](#).
- [50] M. Haque, P. A. McClarty, and I. M. Khaymovich, Entanglement of midspectrum eigenstates of chaotic many-body systems: Reasons for deviation from random ensembles, [Physical Review E **105**, 014109 \(2022\)](#)

METHODS

Computable formula for the 2-norm $\|\hat{X}\|_2^{(A)}$. We derive a formula for the 2-norm $\|\hat{X}\|_2^{(A)}$, which is computable, given an orthonormal basis $\{\hat{\Lambda}_\mu\}_{\mu=1}^M$ of $\mathcal{A} + \mathbb{R}\hat{I}$ with $M := \dim(\mathcal{A} + \mathbb{R}\hat{I})$. For an arbitrary operator \hat{X} , we introduce $\vec{X} = (X_1, X_2, \dots)$ with $X_\mu := \text{tr}(\hat{\Lambda}_\mu^\dagger \hat{X})$. To calculate the supremum in Eq. (1), we use the expansion of $\hat{A} \in \mathcal{A} + \mathbb{R}\hat{I}$ as $\hat{A} = \sum_\mu c_\mu \hat{\Lambda}_\mu$, where $c_\mu = \text{tr}(\hat{\Lambda}_\mu^\dagger \hat{A}) \in \mathbb{R}$. Substituting this expansion in Eq. (1) gives

$$\begin{aligned} \|\hat{X}\|_2^{(A)} &= \sup_{\substack{\hat{A} \in \mathcal{A} + \mathbb{R}\hat{I} \\ \hat{A} \neq 0}} \left| \text{tr} \left(\frac{\hat{A}^\dagger}{\|\hat{A}\|_2} \hat{X} \right) \right| \\ &= \sup_{\vec{c} \in \mathbb{R}^M : \vec{c} \neq 0} \left| \sum_{\mu=1}^M \frac{c_\mu}{\|\vec{c}\|_2} \text{tr}(\hat{\Lambda}_\mu^\dagger \hat{X}) \right| \\ &= \sup_{\vec{c} \in \mathbb{R}^M : \|\vec{c}\|_2=1} \left| \vec{c} \cdot (\text{Re } \vec{X} + i \text{Im } \vec{X}) \right| \\ &= \sup_{\vec{c} \in \mathbb{R}^M : \|\vec{c}\|_2=1} \sqrt{\vec{c}^T \mathcal{Q} \vec{c}}, \end{aligned} \quad (3)$$

where $\mathcal{Q} := (\text{Re } \vec{X})(\text{Re } \vec{X})^T + (\text{Im } \vec{X})(\text{Im } \vec{X})^T$ is a symmetric matrix. Since \mathcal{Q} is at most of rank 2, it is straightforward to obtain the eigenvalues of \mathcal{Q} , and we obtain the following formula:

$$\|\hat{X}\|_2^{(A)} = \sqrt{\frac{\|\vec{X}\|_2^2 + |\vec{X}^T \cdot \vec{X}|}{2}}. \quad (4)$$

Proof of Theorem 1. As explained in the main text, the proof of Theorem 1 consists of the three steps. Before explaining each step, we introduce some notations.

Let $\{|\alpha\rangle\}_{\alpha=1}^D$ be an arbitrarily chosen orthonormal basis of \mathcal{H} . To see the square of the p -norm $f_p^{(\alpha\beta)} := (\|\hat{\rho}_{\alpha\beta} - \hat{\rho}_{\delta E}^{(\text{mc})}(E_\alpha)\delta_{\alpha\beta}\|_p^{(A)})^2$ with $p = 1, 2$ as a function of the energy eigenbasis $\hat{U} := (|E_1\rangle |E_2\rangle \dots) = \sum_{\alpha=1}^D |E_\alpha\rangle\langle\alpha|$, we introduce the operator

$$\hat{\Delta}_I^{(\alpha\beta)} := |\alpha\rangle\langle\beta| - \frac{\delta_{\alpha\beta}}{d_{E_\alpha, \delta E}} \sum_{|E_\gamma\rangle \in \mathcal{H}_{E_\alpha, \delta E}} |\gamma\rangle\langle\gamma|, \quad (5)$$

where $\mathcal{H}_{E_\alpha, \delta E} := \text{span}\{|E_\gamma\rangle \mid |E_\gamma - E_\alpha| < \delta E\}$ is the microcanonical energy shell, and $d_{E_\alpha, \delta E} := \dim \mathcal{H}_{E_\alpha, \delta E}$. Then, we can write $f_p^{(\alpha\beta)}(\hat{U}) = (\|\hat{U} \hat{\Delta}_I^{(\alpha\beta)} \hat{U}^\dagger\|_p^{(A)})^2$. We will drop the superscripts $(\alpha\beta)$ from $f_p^{(\alpha\beta)}(\hat{U})$ and $\hat{\Delta}_I^{(\alpha\beta)}$ whenever they are irrelevant.

Step i): Estimating the average of $f_2^{(\alpha\beta)}$. Here, we estimate the average of $f_2^{(\alpha\beta)}$ over the Haar measure. Substituting the inequality $0 \leq |\vec{X}^T \cdot \vec{X}| \leq \|\vec{X}\|_2^2$ into the formula (4) gives $2^{-1/2} \|\vec{X}_U\|_2 \leq \|\hat{X}\|_2^{(A)} \leq \|\vec{X}_U\|_2$,

where $(\vec{X}_U)_\mu := \text{tr}(\hat{\Lambda}_\mu^\dagger \hat{U} \hat{X} \hat{U}^\dagger)$. The formula for the second-order moments of the Haar measure [43, Corollary 13] yields

$$\mathbb{E} \|\vec{X}_U\|_2^2 = \frac{M-1}{D^2-1} \|\hat{X}\|_2^2 \quad (6)$$

for traceless \hat{X} . In addition, we can calculate

$$\frac{1}{2} \leq \|\hat{\Delta}_I^{(\alpha\beta)}\|_2^2 = 1 - \delta_{\alpha\beta} \frac{1}{d_{E_\alpha, \delta E}} \leq 1. \quad (7)$$

except for the trivial case of $d_{E_\alpha, \delta E} = 1$, which we do not consider. We also have $M/2D^2 \leq (M-1)/(D^2-1) \leq M/D^2$ except for the trivial case of $M=1$, which we do not consider. Therefore, we obtain

$$\frac{1}{8} \frac{M}{D^2} \leq \mathbb{E}[f_2^{(\alpha\beta)}] \leq \frac{M}{D^2}. \quad (8)$$

From the inequality $\|\cdot\|_2^{(A)} \leq \|\cdot\|_1^{(A)} \leq \sqrt{D} \|\cdot\|_2^{(A)}$, we also obtain

$$\frac{1}{8} \frac{M}{D^2} \leq \mathbb{E}[f_1^{(\alpha\beta)}] \leq \frac{M}{D}. \quad (9)$$

Step ii): Lipschitz continuity of $f_p^{(\alpha\beta)}(\hat{U})$.

To derive an inequality for $(\Lambda_p^{(\hat{H}, A)})^2 = \max_{|E_\alpha\rangle, |E_\beta\rangle \in \mathcal{H}_{E_\alpha, \Delta}} f_p^{(\alpha\beta)}(\hat{U})$ with $p = 1, 2$, we employ the concentration inequality for the Haar measure [41–43], which applies to any Lipschitz continuous function of \hat{U} . We here show the Lipschitz continuity of $f_p^{(\alpha\beta)}(\hat{U})$ before introducing the concentration inequality.

We start with showing the Lipschitz continuity of the inner product $\text{tr}(\hat{A} \hat{U} \hat{X} \hat{U}^\dagger)$ for any \hat{A} and \hat{X} that are independent of \hat{U} . By denoting $\delta\hat{U} := \hat{U}_1 - \hat{U}_2$ and setting $(p, q) = (1, \infty)$ or $(2, 2)$, this follows from the Hölder inequality and the triangle inequality as

$$\begin{aligned} & \left| \text{tr}(\hat{A} \hat{U}_1 \hat{X} \hat{U}_1^\dagger) - \text{tr}(\hat{A} \hat{U}_2 \hat{X} \hat{U}_2^\dagger) \right| \\ & \leq \|\hat{A}\|_q \|\hat{U}_1 \hat{X} \hat{U}_1^\dagger - \hat{U}_2 \hat{X} \hat{U}_2^\dagger\|_p \\ & = \|\hat{A}\|_q \|\delta\hat{U} \hat{X} \delta\hat{U}^\dagger + \delta\hat{U} \hat{X} \hat{U}_2^\dagger + \hat{U}_2 \hat{X} \delta\hat{U}^\dagger\|_p \\ & \leq \|\hat{A}\|_q \left(\|\delta\hat{U} \hat{X} \delta\hat{U}^\dagger\|_p + \|\delta\hat{U} \hat{X} \hat{U}_2^\dagger\|_p + \|\hat{U}_2 \hat{X} \delta\hat{U}^\dagger\|_p \right) \\ & \leq \|\hat{A}\|_q \|\delta\hat{U}\|_2 \left(\|\hat{X} \delta\hat{U}^\dagger\|_2 + \|\hat{X} \hat{U}_2^\dagger\|_2 + \|\hat{U}_2 \hat{X}\|_2 \right) \\ & \leq \|\hat{A}\|_q \|\delta\hat{U}\|_2 \|\hat{X}\|_2 \left(\|\delta\hat{U}\|_\infty + 2\|\hat{U}_1\|_\infty \right) \\ & \leq 4\|\hat{X}\|_2 \|\hat{A}\|_q \|\hat{U}_1 - \hat{U}_2\|_2. \end{aligned} \quad (10)$$

Since $|\max_x g(x) - \max_x h(x)| \leq \max_x |g(x) - h(x)|$ for any functions g and h , we conclude from Eq. (10) that the p -norm $\|\hat{U} \hat{X} \hat{U}^\dagger\|_p^{(A)}$ ($p = 1, 2$) is Lipschitz continuous with the Lipschitz constant no larger than $4\|\hat{X}\|_2$. Moreover, the Hölder inequality implies $\|\hat{U} \hat{X} \hat{U}^\dagger\|_p^{(A)} \leq \|\hat{X}\|_p$.

Taking Eq. (7) and $\|\hat{\Delta}_I\|_1 \leq 2$ into account, we conclude

$$\begin{aligned} \left| f_p(\hat{U}_1) - f_p(\hat{U}_2) \right| &\leq 2 \|\hat{\Delta}_I\|_p \left| f_2(\hat{U}_1)^{\frac{1}{2}} - f_2(\hat{U}_2)^{\frac{1}{2}} \right| \\ &\leq 8 \|\hat{\Delta}_I\|_p \|\hat{\Delta}_I\|_2 \|U_1 - U_2\|_2 \\ &\leq 16 \|U_1 - U_2\|_2, \end{aligned} \quad (11)$$

which shows that $f_p^{(\alpha\beta)}(\hat{U})$ ($p = 1, 2$) is Lipschitz continuous with Lipschitz constant no larger than 16. This fact is independent of the indices $(\alpha\beta)$.

Step iii): Applying the concentration inequality of the Haar measure. The concentration of the Haar measure on $\text{SU}(D)$ means the following [41–43]; for any $\delta > 0$ that can be D -dependent and any Lipschitz continuous function f on $\text{SU}(D)$ with Lipschitz constant η_f , the following inequalities hold:

$$\mathbb{P} \left[f(\hat{U}) \geq \mathbb{E}_{\hat{U}}[f] + \delta \right] \leq \exp \left[-\frac{\delta^2 D}{4\eta_f^2} \right] \quad (12)$$

$$\text{and } \mathbb{P} \left[f(\hat{U}) \leq \mathbb{E}_{\hat{U}}[f] - \delta \right] \leq \exp \left[-\frac{\delta^2 D}{4\eta_f^2} \right], \quad (13)$$

where $\mathbb{E}_{\hat{U}}$ denotes the average over the Haar measure for \hat{U} . For a family of Lipschitz functions, we can derive the following lemma.

Lemma 1. *Let \mathcal{I} be a finite set of indices and $\{f_j(\hat{U})\}_{j \in \mathcal{I}}$ be a family of Lipschitz functions on $\text{SU}(D)$ with Lipschitz constant no larger than η , which is independent of the indices $j \in \mathcal{I}$. Suppose that there exist constants C_{\min} and C_{\max} that are independent of j and satisfy $C_{\min} \leq \mathbb{E}f_j \leq C_{\max}$ for all $j \in \mathcal{I}$. Then, for arbitrary $\delta > 0$, we have*

$$C_{\min} - \delta \leq \max_{j \in \mathcal{I}} f_j(\hat{U}) \leq C_{\max} + \delta \quad (14)$$

for a set of \hat{U} whose probability measure is no smaller than $1 - 2|\mathcal{I}| \exp[-\delta^2 D/4\eta^2]$.

Proof. Since $\max_{j \in \mathcal{I}} f_j(\hat{U}) \geq C_{\max} + \delta$ implies that there exists at least one $j' \in \mathcal{I}$ such that $f_{j'}(\hat{U}) \geq C_{\max} + \delta$, we obtain

$$\begin{aligned} \mathbb{P} \left[\max_{j \in \mathcal{I}} f_j \geq C_{\max} + \delta \right] &\leq \sum_{j \in \mathcal{I}} \mathbb{P} \left[f_j \geq C_{\max} + \delta \right] \\ &\leq \sum_{j \in \mathcal{I}} \mathbb{P} \left[f_j \geq \mathbb{E}f_j + \delta \right] \\ &\leq |\mathcal{I}| \exp \left[-\frac{\delta^2 D^2}{4\eta^2} \right]. \end{aligned} \quad (15)$$

where we use $\mathbb{E}f_j \leq C_{\max}$ in deriving the second inequality, and use the inequality (12) in deriving the last inequality. In a similar manner, we obtain

$$\mathbb{P} \left[\max_{j \in \mathcal{I}} f_j \leq C_{\min} - \delta \right] \leq |\mathcal{I}| \exp \left[-\frac{\delta^2 D^2}{4\eta^2} \right]. \quad (16)$$

The equations (15) and (16) complete the proof of Lemma 1. \blacksquare

Let \mathcal{I} be a set of indices $(\alpha\beta)$ such that $|E_\alpha\rangle, |E_\beta\rangle \in \mathcal{H}_{E,\Delta}$ and consider the families of Lipschitz functions $\{f_p^{(\alpha\beta)}\}_{(\alpha\beta) \in \mathcal{I}}$ with $p = 1, 2$. We have bounds on $\mathbb{E}[f_p^{(\alpha\beta)}]$ independent of the indices $(\alpha\beta) \in \mathcal{I}$ in Eqs. (8) and (9) and showed the Lipschitz continuity of $f_p^{(\alpha\beta)}$ in Eq. (11). Therefore, we can apply Lemma 1 to the families $\{f_p^{(\alpha\beta)}\}_{(\alpha\beta) \in \mathcal{I}}$ with $p = 1, 2$. Since $\delta > 0$ is arbitrary, we can choose $\delta = cD^\epsilon/\sqrt{D}$ for any positive D -independent constants $\epsilon > 0$ and $c > 0$. The inequality (14) with this choice of δ implies that

$$\frac{1}{8} \frac{M}{D^2} - c \frac{D^\epsilon}{\sqrt{D}} \leq (\Lambda_2^{\langle \hat{H}, \mathcal{A} \rangle})^2 \leq \frac{M}{D^2} + c \frac{D^\epsilon}{\sqrt{D}}, \quad (17)$$

$$\frac{1}{8} \frac{M}{D^2} - c \frac{D^\epsilon}{\sqrt{D}} \leq (\Lambda_1^{\langle \hat{H}, \mathcal{A} \rangle})^2 \leq \frac{M}{D^2} + c \frac{D^\epsilon}{\sqrt{D}}, \quad (18)$$

for sets of \hat{U} whose probability measure is no smaller than $1 - 2|\mathcal{I}| \exp[-\frac{c^2 D^{2\epsilon}}{1024}]$. This is the precise meaning of the inequality (2) in the main text. Here, we have

$$|\mathcal{I}| \exp \left[-\frac{c^2 D^{2\epsilon}}{1024} \right] \leq \exp \left[-\frac{c^2 D^{2\epsilon}}{1024} + 2 \log D \right] = e^{-\mathcal{O}(D^{2\epsilon})}, \quad (19)$$

where we use $|\mathcal{I}| \leq D^2$. This is the precise meaning of the statement “for almost all $\hat{H} \in \mathcal{G}_{\text{inv}}$ ” below the inequality (2) in the main text.

Proof of Theorem 2 for spin systems. For spin- S systems, the m -body operator space is defined as

$$\mathcal{A}_N^{[0,m]} := \bigoplus_{\vec{m}=0}^m \text{span} \left\{ \hat{\sigma}_{x_1}^{(p_1)} \dots \hat{\sigma}_{x_{\vec{m}}}^{(p_{\vec{m}})} \mid \begin{array}{l} 1 \leq x_1 \leq \dots \leq x_{\vec{m}} \leq V \\ 1 \leq p_j < d_{\text{loc}}^2 \end{array} \right\}. \quad (20)$$

Its dimension is calculated to be

$$\dim \mathcal{A}_N^{[0,m]} = D^2 \sum_{j=0}^m P_j, \quad (21)$$

where $D_N := \dim \mathcal{H}_N = (d_{\text{loc}})^N$, and $P_j := \binom{N}{j} \frac{(d_{\text{loc}}^2 - 1)^j}{d_{\text{loc}}^{2N}}$ with $d_{\text{loc}} := 2S + 1$ is the probability mass for the binomial distribution $\mathcal{B}(N, p)$ with $p = 1 - (d_{\text{loc}})^{-2}$. As a property of the binomial distribution, we have $P_{m-1} < P_m$ for $m < (N+1)p$. Therefore, we have $\dim \mathcal{A}_N^{[0,m]} \leq (m+1)P_m$ for $m/N < p$.

To derive the lower bound α_L , we apply the Stirling’s formula to P_m , obtaining

$$\frac{\dim \mathcal{A}_N^{[0,m]}}{D_N} \leq \exp \left[NG \left(\frac{m}{N} \right) + \mathcal{O}(\log N) \right] \quad (22)$$

for $m/N < p$, where $G(x) := H(x) + x \log(d_{\text{loc}}^2 - 1) - \log d_{\text{loc}}$, and $H(x) = -x \log x - (1-x) \log(1-x)$. Here, we define α_L as a root of $G(x)$. Because $G(0) = -\log d_{\text{loc}} < 0$, and

$$G\left(\frac{1}{2}\right) = \frac{1}{2} \log 4 \left(1 - \frac{1}{d_{\text{loc}}^2} \right), \quad (23)$$

which is positive for $d_{\text{loc}} \geq 2$, we conclude $\alpha_L \in (0, 1/2)$. Moreover, it is straightforward to show that $G(x) < 0$ for $x < \alpha_L$. Therefore, the ETH measure decays exponentially with increasing the system size when $m/N < \alpha_L$ as claimed in Theorem 2 in the main text.

To derive the upper bound α_U , we use the fact that $\mathcal{B}(N, p)$ converges in distribution to a Gaussian distribution $\mathcal{N}(Np, Np(1-p))$ for large N . This implies that $\dim \mathcal{A}_N^{[0, Np]}/D_N^2$ converges to $1/2$ for large N . Then, Theorem 1 implies $\alpha_U = p = 1 - (d_{\text{loc}})^{-2}$ for spin systems.

Proof of Theorem 2 for Bose and Fermi systems. For N -particle Bose and spinless Fermion systems on a V -site lattice, the m -body operator space is defined as

$$\mathcal{A}_{N,V}^{[0,m]} := \left\{ \hat{A} + \hat{A}^\dagger, i(\hat{A} - \hat{A}^\dagger) \mid \hat{A} \in \tilde{\mathcal{A}}_{N,V}^{[0,m]} \right\}, \quad (24)$$

where

$$\tilde{\mathcal{A}}_{N,V}^{[0,m]} := \text{span} \left\{ \hat{a}_{x_1}^\dagger \cdots \hat{a}_{x_m}^\dagger \hat{a}_{y_1} \cdots \hat{a}_{y_m} \mid \begin{array}{l} 1 \leq x_j \leq V \\ 1 \leq y_j \leq V \end{array} \right\}. \quad (25)$$

Here, \hat{a} denotes the Boson annihilation operator \hat{b} or the Fermion annihilation operator \hat{f} , and we recall that we consider the Hilbert space with definite a particle number as

$$\mathcal{H}_{N,V} = \text{span} \left\{ \hat{a}_{x_1}^\dagger \cdots \hat{a}_{x_N}^\dagger |0\rangle \mid 1 \leq x_j \leq V \right\}. \quad (26)$$

While the numbers of annihilation and creation operators are both required to be equal to m in Eq. (25), we can show that the space $\tilde{\mathcal{A}}_{N,V}^{[0,m]}$ includes $\tilde{\mathcal{A}}_{N,V}^{[0,m-1]}$ so that $\tilde{\mathcal{A}}_{N,V}^{[0,m-1]} \subset \tilde{\mathcal{A}}_{N,V}^{[0,m]}$. This is because the particle-number conservation makes the particle number operator $\hat{N} := \sum_{x=1}^N \hat{a}_x^\dagger \hat{a}_x$ essentially proportional to the identity operator. Indeed, by denoting the projection operator onto $\mathcal{H}_{N,V}$ by $\hat{\Pi}_{N,V}$, we have

$$\begin{aligned} & \hat{\Pi}_{N,V}(\hat{a}_{x_1}^\dagger \cdots \hat{a}_{x_{m-1}}^\dagger \hat{a}_{y_1} \cdots \hat{a}_{y_{m-1}}) \hat{\Pi}_{N,V} \\ &= \hat{\Pi}_{N,V}(\hat{a}_{x_1}^\dagger \cdots \hat{a}_{x_{m-1}}^\dagger \frac{\hat{N}}{N-m+1} \hat{a}_{y_1} \cdots \hat{a}_{y_{m-1}}) \hat{\Pi}_{N,V} \\ &\propto \sum_{x_m=1}^V \hat{\Pi}_{N,V}(\hat{a}_{x_1}^\dagger \cdots \hat{a}_{x_{m-1}}^\dagger \hat{a}_{x_m}^\dagger \hat{a}_{x_m} \hat{a}_{y_1} \cdots \hat{a}_{y_{m-1}}) \hat{\Pi}_{N,V}, \end{aligned} \quad (27)$$

which proves $\mathcal{A}_{N,V}^{[0,m-1]} \subset \mathcal{A}_{N,V}^{[0,m]}$.

Proof of Theorem 2 for Bose systems. The dimension of the m -body operator space is calculated to be $\dim \mathcal{A}_{N,V}^{[0,m]} = \binom{V+m-1}{m}^2$, while that of the Hilbert space is given by $D_{N,V} = \dim \mathcal{H}_{N,V} = \binom{V+N-1}{N}$.

To derive the lower bound α_L , we apply the Stirling's formula, obtaining

$$\frac{\dim \mathcal{A}_{N,V}^{[0,m]}}{D} = \exp \left[VG \left(\frac{m}{N} \right) + \mathcal{O}(\log V) \right], \quad (28)$$

where $G(x) := 2(1+nx)H((1+nx)^{-1}) - (1+n)H((1+n)^{-1})$ with $n := N/V$. Here, $G(x)$ is a monotonically increasing function of x , and we define α_L as a root of $G(x)$. Then, we have $G(0) = -(1+n)H((1+n)^{-1}) < 0$ and

$$G \left(\frac{1}{2} \right) = \log \frac{(1+\frac{n}{2})^2}{1+n} + n \log \frac{2+n}{1+n} > 0. \quad (29)$$

Therefore, we conclude $\alpha_L \in (0, 1/2)$. Since $G(x)$ is monotonically increasing, we have $G(x) < 0$ for $x < \alpha_L$. Therefore, the ETH measure decays exponentially in the system size when $m/N < \alpha_L$ as claimed in Theorem 2 in the main text. For Bose systems, the lower bound in Eq. (2) does not give a bound better than the trivial one, i.e., $\alpha_U = 1$.

Proof of Theorem 2 for spinless Fermi systems.

To calculate the dimension of $\mathcal{A}_{N,V}^{[0,m]}$, we consider the particle-hole transformation \hat{C} defined by $\hat{C} \hat{f}_x \hat{C}^\dagger = \hat{f}_x^\dagger$ and $\hat{C} |0\rangle = \hat{f}_1^\dagger \cdots \hat{f}_V^\dagger |0\rangle$. Then, we have

$$\begin{aligned} & \hat{C} \hat{\Pi}_{N,V}(\hat{f}_{x_1}^\dagger \cdots \hat{f}_{x_m}^\dagger \hat{f}_{y_1} \cdots \hat{f}_{y_m}) \hat{\Pi}_{N,V} \hat{C}^\dagger \\ &= \hat{\Pi}_{V-N,V}(\hat{f}_{x_1} \cdots \hat{f}_{x_m} \hat{f}_{y_1}^\dagger \cdots \hat{f}_{y_m}^\dagger) \hat{\Pi}_{V-N,V}. \end{aligned} \quad (30)$$

Since exchanging the order of operators $\hat{f}_{x_1} \cdots \hat{f}_{x_m}$ and $\hat{f}_{y_1}^\dagger \cdots \hat{f}_{y_m}^\dagger$ results in additional terms of at most $(m-1)$ -body ones, Eq. (30) implies $\dim \mathcal{A}_{N,V}^{[0,m]} = \dim(\hat{C} \mathcal{A}_{N,V}^{[0,m]} \hat{C}^\dagger) \leq \dim \mathcal{A}_{V-N,V}^{[0,m]}$ for $m \leq \min\{N, V-N\}$. By setting $N \mapsto V-N$ in the above argument, we obtain the reversed inequality. Therefore, we arrive at

$$\dim \mathcal{A}_{N,V}^{[0,m]} = \dim \mathcal{A}_{V-N,V}^{[0,m]} \quad (31)$$

for $m \leq \min\{N, V-N\}$. This relation combined with the inclusion relation $\mathcal{A}_{N,V}^{[0,m-1]} \subset \mathcal{A}_{N,V}^{[0,m]} \subset \mathcal{L}(\mathcal{H})$ gives $\dim \mathcal{A}_{N,V}^{[0,m]} = D_{N,V}^2$ for $m \geq \min\{N, V-N\}$. Because of Eq. (31), the remaining task is to calculate $\dim \mathcal{A}_{N,V}^{[0,m]}$ for $N/V < 1/2$. In this case, there are $\binom{V}{N}$ choices for both $\{x_1, \dots, x_m\}$ and $\{y_1, \dots, y_m\}$ to have nonzero basis operators. We can show that different choices for these indices give linearly independent basis operators. (See Supplementary Information III for the proof.) Therefore, the dimension of the m -body operator space is calculated to be $\dim \mathcal{A}_{N,V}^{[0,m]} = \binom{V}{\min\{m, V-N\}}^2$, while that of the Hilbert space is given by $D_{N,V} = \dim \mathcal{H}_{N,V} = \binom{V}{N}$.

To derive the lower bound α_L , we apply Stirling's formula, obtaining

$$\frac{\dim \mathcal{A}_{N,V}^{[0,m]}}{D} = \exp \left[VG \left(\frac{m}{N} \right) + \mathcal{O}(\log V) \right], \quad (32)$$

where we set $n := N/V (\leq 1)$ and

$$G(x) := \begin{cases} 2H(nx) - H(n) & (x \leq \frac{1-n}{n}); \\ H(n) & (x > \frac{1-n}{n}). \end{cases} \quad (33)$$

Here, $G(x)$ is a monotonically increasing function of x , and we define α_L as a root of $G(x)$. Then, we have $G(0) = -H(n) < 0$ and

$$G\left(\frac{1}{2}\right) = \begin{cases} \int_0^n \log \frac{2-s}{1-s} ds & (n \leq 2/3); \\ H(n) & (n > 2/3), \end{cases} \quad (34)$$

which is positive. Therefore, we conclude $\alpha_L \in (0, 1/2)$. Since $G(x)$ is monotonically increasing, we have $G(x) < 0$ for $x < \alpha_L$. Therefore, the ETH measure decays exponentially with increasing the system size for $m/N < \alpha_L$ as claimed in Theorem 2 in the main text.

To derive the lower bound α_L , we use $\dim \mathcal{A}_{N,V}^{[0,m]} = D^2$ when $m \geq \min\{N, V - N\}$. Dividing both sides with N shows that we can take $\alpha_U = \min\{1, (1-n)/n\}$. This completes the proof of Theorem 2.

Setup of the numerical calculation. In the numerical calculations, we consider the following ensembles of spin, Bose, and Fermi systems with local and few-body interactions on a one-dimensional lattice. We adopt periodic boundary conditions.

For spin systems, we consider the ensemble of Hamiltonians consisting of 2-local terms, i.e., those given by

$$\hat{H} := \sum_{\alpha, \beta=0}^{d_{\text{loc}}^2-1} J_{\alpha\beta} \left(\sum_{j=1}^V \hat{\sigma}_j^{(\alpha)} \hat{\sigma}_{j+1}^{(\beta)} \right), \quad (35)$$

where $\{\hat{\sigma}_j^{(\alpha)}\}_{\alpha=0}^{d_{\text{loc}}^2-1}$ is an orthonormal basis of the operator space acting on the j th spin with $\hat{\sigma}_j^{(0)}$ being proportional to the identity, and the coefficients $\{J_{\alpha\beta}\}_{\alpha, \beta=0}^{d_{\text{loc}}^2-1}$ are i.i.d. Gaussian random variables with zero mean and unit variance. Since the Hamiltonian (35) has a translation symmetry, we restrict ourselves to the zero-momentum sector in numerical calculations.

For Bose and Fermi systems, we consider the ensemble of Hamiltonians consisting of 3-local and 2-body terms, i.e., those given by $\hat{H} := (\hat{H} + \hat{H}^\dagger + \hat{P}\hat{H}\hat{P} + \hat{P}\hat{H}^\dagger\hat{P})/4$, where \hat{P} is the reflection operator defined by $\hat{P}\hat{a}_j\hat{P} = \hat{a}_{V-j+1}$ with \hat{a}_j being bosonic or fermionic annihilation operator acting on site j , and

$$\tilde{\hat{H}} := \sum_{x_1, x_2, y_1, y_2=1}^3 J_{x_1 x_2}^{y_1 y_2} \left(\sum_{j=1}^V \hat{a}_{j+x_1}^\dagger \hat{a}_{j+x_2}^\dagger \hat{a}_{j+y_1} \hat{a}_{j+y_2} \right). \quad (36)$$

Here, the coefficients $\{J_{x_1 x_2}^{y_1 y_2}\}_{x_1, x_2, y_1, y_2=1}^3$ are i.i.d. complex Gaussian random variables satisfying $\mathbb{E} J_{x_1 x_2}^{y_1 y_2} = 0$, $\mathbb{E} |J_{x_1 x_2}^{y_1 y_2}|^2 = 1$, and $\mathbb{E} (J_{x_1 x_2}^{y_1 y_2})^2 = 0$. Since the Hamiltonian \hat{H} has translation and reflection symmetries, we restrict ourselves to the zero-momentum and even-parity sector in numerical calculations. The filling factor ($n := N/V$) is set to $n = 1$ for Bose systems and $n = 1/2$ for Fermi systems.

DATA AVAILABILITY

The numerical data plotted in the figures of this Article are available from the authors upon reasonable request.

CODE AVAILABILITY

The source codes used in the numerical calculations are available from the authors upon reasonable request.

ACKNOWLEDGMENTS

We are grateful to Takashi Mori for the discussions about the relation of our results to the previous ones. S.S. is also grateful to Masaya Nakagawa for the valuable and helpful discussions on the dimension counting of the m -body space for Fermi systems. This work was supported by KAKENHI Grant Numbers JP22H01152 from the Japan Society for the Promotion of Science (JSPS). S.S. was supported by KAKENHI Grant Number JP22J14935 from the Japan Society for the Promotion of Science (JSPS) and Forefront Physics and Mathematics Program to Drive Transformation (FoPM), a World-leading Innovative Graduate Study (WINGS) Program, the University of Tokyo. R.H. was supported by JST ERATO-FS Grant Number JPMJER2204, Japan. M.U. is supported by the CREST program ‘‘Quantum Frontiers’’ (Grant No. JPMJCR2311) by the Japan Science and Technology Agency.

COMPETING INTERESTS

The authors declare no competing interests.

AUTHOR CONTRIBUTIONS

All authors contributed to the manuscript writing and the discussion and interpretation of the analytical results and the numerical data. S.S. conceived the idea, mainly carried out the analytical calculations, conducted all the numerical calculations, and drafted the manuscript. R.H. also gave insights into the analytical calculations. R.H. and M.U. greatly contributed to the improvement of the manuscript. M.U. supervised the work.

Supplementary Information:

Bounds on eigenstate thermalization

Shoki Sugimoto,^{1,*} Ryusuke Hamazaki,^{1,2} and Masahito Ueda^{3,4}

¹*Nonequilibrium Quantum Statistical Mechanics RIKEN Hakubi Research Team,
RIKEN Cluster for Pioneering Research (CPR), Wako, Saitama 351-0198, Japan*

²*RIKEN iTHEMS, Wako, Saitama 351-0198, Japan*

³*Department of Physics, The University of Tokyo,
7-3-1 Hongo, Bunkyo-ku, Tokyo 113-0033, Japan*

⁴*RIKEN Center for Emergent Matter Science (CEMS), Wako 351-0198, Japan*

(Dated: December 17, 2024)

CONTENTS

I. Scaling behavior of the normalization constant $\ \hat{A}\ _q$	13
II. $\ \cdot\ _1^{(A)}$ as a unified measure for quantum-thermal equilibrium	14
A. Subsystem thermal equilibrium	14
B. Microscopic thermal equilibrium (MITE) [1–3]	14
C. Macroscopic thermal equilibrium (MATE) [1–3]	15
III. Linear independence of basis operators for the m -body operator space	18
IV. Narrowing the operator space where an ETH-breaking operator typically exists for systems with Haar-distributed energy eigenstates	20
V. Details on the numerical calculations	22
VI. Energy dependence of the bounds on the ratio m_*/N	25
VII. Numerical results for concrete physical models	28
References	31

I. SCALING BEHAVIOR OF THE NORMALIZATION CONSTANT $\|\hat{A}\|_q$

Here, we demonstrate that the quantity $\hat{A}/\|\hat{A}\|_q$ in the definition of $\|\cdot\|_1^{(\mathcal{A})}$ in Eq. (3) in the main text is thermodynamically intensive only for $q = \infty$. We first derive the N -dependence of the normalization constant $\|\hat{A}\|_q$ for an extensive operator $\hat{M}_z := \sum_{j=1}^N \hat{\sigma}_j^{(z)}$, where $\hat{\sigma}^{(z)}$ is the Pauli z -operator. The eigenstates of \hat{M}_z are given by tensor products of those of $\hat{\sigma}^{(z)}$, and the eigenvalues are given by $-N + 2j$ ($j = 0, \dots, N$), where j is the number of spins where the local state is the eigenstate of $\hat{\sigma}^{(z)}$ with eigenvalue $+1$. Therefore, we have

$$\begin{aligned} \|\hat{M}_z\|_q^q &= \sum_{j=0}^N \binom{N}{j} |-N + 2j|^q \\ &= N^q \sum_{j=0}^N \left| -1 + 2\frac{j}{N} \right|^q \exp \left[NH \left(\frac{j}{N} \right) + \frac{1}{2} \log \frac{N}{2\pi j(N-j)} + \mathcal{O}(N^{-1}) \right], \end{aligned} \quad (\text{S1})$$

where $H(x) := -x \log x - (1-x) \log(1-x)$ is the binary entropy.

Since we are interested in the N -dependence of $\|\hat{M}_z\|_q$ for large N , the sum in Eq. (S1) can be replaced by the integral:

$$\begin{aligned} \|\hat{M}_z\|_q^q &\simeq N^{q+1} \int_0^1 dx |-1 + 2x|^q \exp \left[NH(x) - \frac{1}{2} \log(x(1-x)) - \frac{1}{2} \log(2\pi N) + \mathcal{O}(N^{-1}) \right] \\ &\simeq \frac{N^{q+\frac{1}{2}}}{\sqrt{2\pi}} \int_0^1 dx |-1 + 2x|^q \exp \left[NH(x) - \frac{1}{2} \log(x(1-x)) + \mathcal{O}(N^{-1}) \right] \\ &\simeq \frac{N^{q+\frac{1}{2}}}{\sqrt{2\pi}} \int_{-\frac{1}{2}}^{\frac{1}{2}} dx |2x|^q \exp \left[NH \left(\frac{1}{2} + x \right) - \frac{1}{2} \log \left(\frac{1}{4} - x^2 \right) + \mathcal{O}(N^{-1}) \right]. \end{aligned} \quad (\text{S2})$$

We then apply the saddle point method to Eq. (S2), obtaining

$$\begin{aligned} \|\hat{M}_z\|_q^q &\simeq \frac{N^{q+\frac{1}{2}}}{\sqrt{2\pi}} \int_{-\frac{1}{2}}^{\frac{1}{2}} dx |2x|^q \exp \left[N \log 2 - \frac{4Nx^2}{2} + \log 2 + \frac{x^2}{2} + \mathcal{O}(x^4, N^{-1}) \right] \\ &= 2^N \frac{N^{\frac{q}{2}}}{\sqrt{2\pi}} \int_{-\sqrt{N}}^{\sqrt{N}} dx |x|^q \exp \left[-\frac{x^2}{2} + \mathcal{O}(N^{-1}) \right] \\ &\simeq 2^N \frac{N^{\frac{q}{2}}}{\sqrt{2\pi}} \int_{-\infty}^{+\infty} dx |x|^q \exp \left[-\frac{x^2}{2} \right] \\ &= 2^N N^{\frac{q}{2}} \frac{2^{\frac{q}{2}}}{\sqrt{\pi}} \Gamma \left(\frac{q+1}{2} \right). \end{aligned} \quad (\text{S3})$$

Therefore, for any fixed q and sufficiently large N , the normalization constant $\|\hat{M}_z\|_q$ scales as $\sim \sqrt{N} 2^{\frac{N}{q}}$ and hence $\hat{M}_z/\|\hat{M}_z\|_q$ is thermodynamically intensive only for $q = \infty$.

II. $\|\cdot\|_1^{(\mathcal{A})}$ AS A UNIFIED MEASURE FOR QUANTUM-THERMAL EQUILIBRIUM

As mentioned in the main text, the seminorm $\|\cdot\|_1^{(\mathcal{A})}$ with an apt choice of \mathcal{A} serves as a unified measure for various notions about quantum thermal equilibrium. In this section, we provide some examples.

A. Subsystem thermal equilibrium

For any subsystem \mathcal{S} and any $\hat{A}_{\mathcal{S}} \otimes \text{id}_{\mathcal{S}^c} \in \mathcal{L}(\mathcal{H}_{\mathcal{S}}) \otimes \text{id}_{\mathcal{S}^c}$, we have $\|\hat{A}_{\mathcal{S}} \otimes \text{id}_{\mathcal{S}^c}\|_{\infty} = \|\hat{A}_{\mathcal{S}}\|_{\infty}$. By setting $\mathcal{A} = \mathcal{L}(\mathcal{H}_{\mathcal{S}}) \otimes \text{id}_{\mathcal{S}^c}$, we have

$$\begin{aligned} \|\hat{X}\|_1^{(\mathcal{A})} &= \max_{\hat{A} \in \mathcal{L}(\mathcal{H}_{\mathcal{S}}) \otimes \text{id}_{\mathcal{S}^c}} \left| \text{tr} \left(\frac{\hat{A}}{\|\hat{A}\|_{\infty}} \hat{X} \right) \right| \\ &= \max_{\hat{A}_{\mathcal{S}} \in \mathcal{L}(\mathcal{H}_{\mathcal{S}})} \left| \text{tr} \left(\frac{\hat{A}_{\mathcal{S}}}{\|\hat{A}_{\mathcal{S}}\|_{\infty}} \text{tr}_{\mathcal{S}^c}(\hat{X}) \right) \right| \\ &= \left\| \text{tr}_{\mathcal{S}^c}(\hat{X}) \right\|_1. \end{aligned} \quad (\text{S4})$$

Thus, the seminorm $\|\cdot\|_1^{(\mathcal{A})}$ reduces to the trace norm on a subsystem \mathcal{S} for $\mathcal{A} = \mathcal{L}(\mathcal{H}_{\mathcal{S}}) \otimes \text{id}_{\mathcal{S}^c}$, and the smallness of $\|\hat{\sigma} - \hat{\rho}_{\text{th}}\|_1^{(\mathcal{A})}$ for a thermal ensemble $\hat{\rho}_{\text{th}}$ ensures that quantum states $\hat{\sigma}$ are in thermal equilibrium in a subsystem \mathcal{S} .

B. Microscopic thermal equilibrium (MITE) [1–3]

The notion of microscopic thermal equilibrium (MITE) is introduced in Refs. [1, 2] as follows.

Definition II.1: Microscopic thermal equilibrium (MITE) [2]

A state $\hat{\sigma}$ is said to be in microscopic thermal equilibrium (MITE) on a length scale l_0 if it satisfies

$$\left\| \text{tr}_{\mathcal{S}^c}(\hat{\sigma}) - \text{tr}_{\mathcal{S}^c}(\hat{\rho}_{\text{th}}) \right\|_1 < \epsilon \quad (\text{S5})$$

for every subsystem \mathcal{S} with $\text{Diam}(\mathcal{S}) \leq l_0$, where $\epsilon \ll 1$ and the diameter of \mathcal{S} is defined by $\text{Diam}(\mathcal{S}) := \sup_{x,y \in \mathcal{S}} d(x,y)$ for some distance measure d .

As mentioned in Ref. [2], MITE can be regarded as the thermal equilibrium relative to

$$\mathcal{A}_{\text{MITE}} = \bigcup_{\mathcal{S}: \text{Diam}(\mathcal{S}) \leq l_0} \mathcal{L}(\mathcal{H}_{\mathcal{S}}) \otimes \text{id}_{\mathcal{S}^c}. \quad (\text{S6})$$

Then, we have the following proposition.

Proposition II.1

Let $\hat{\sigma}$ be an arbitrary quantum state and $\hat{\rho}_{\text{th}}$ be a thermal ensemble. Then,

$$\hat{\sigma} \text{ is in MITE} \iff \|\hat{\sigma} - \hat{\rho}_{\text{th}}\|_1^{(\mathcal{A}_{\text{MITE}})} \leq \epsilon, \quad (\text{S7})$$

where $\epsilon \ll 1$.

Proof. The proof follows immediately from the following equation:

$$\begin{aligned} \|\hat{\sigma} - \hat{\rho}_{\text{th}}\|_1^{(\mathcal{A}_{\text{MITE}})} &= \max_{\hat{A} \in \mathcal{A}_{\text{MITE}}} \left| \text{tr} \left(\frac{\hat{A}}{\|\hat{A}\|_\infty} (\hat{\sigma} - \hat{\rho}_{\text{th}}) \right) \right| \\ &= \max_{\mathcal{S}: \text{Diam}(\mathcal{S}) \leq l_0} \max_{\hat{A}_{\mathcal{S}} \in \mathcal{L}(\mathcal{H}_{\mathcal{S}})} \left| \text{tr}_{\mathcal{S}} \left(\frac{\hat{A}_{\mathcal{S}}}{\|\hat{A}_{\mathcal{S}}\|_\infty} (\text{tr}_{\mathcal{S}^c}(\hat{\sigma}) - \text{tr}_{\mathcal{S}^c}(\hat{\rho}_{\text{th}})) \right) \right| \\ &= \max_{\mathcal{S}: \text{Diam}(\mathcal{S}) \leq l_0} \|\text{tr}_{\mathcal{S}^c}(\hat{\sigma}) - \text{tr}_{\mathcal{S}^c}(\hat{\rho}_{\text{th}})\|_1. \end{aligned} \quad (\text{S8})$$

■

Mori et al. [3] extend the notion of MITE by replacing the spatial constraints $\text{Diam}(\mathcal{S}) \leq l_0$ with a “few-body” constraint as $|\mathcal{S}| = k$ with an integer k of $\mathcal{O}(1)$, i.e., they consider

$$\mathcal{A}_{\text{MITE}}^{(\text{few})} = \bigcup_{\mathcal{S}: |\mathcal{S}|=k} \mathcal{L}(\mathcal{H}_{\mathcal{S}}) \otimes \text{id}_{\mathcal{S}^c} \quad (\text{S9})$$

in addition to $\mathcal{A}_{\text{MITE}}$. The same proof for Proposition II.1 applies to the MITE with respect to $\mathcal{A}_{\text{MITE}}^{(\text{few})}$, and we have the following proposition:

Proposition II.2

Let $\hat{\sigma}$ be an arbitrary quantum state and $\hat{\rho}_{\text{th}}$ be a thermal ensemble. Then,

$$\hat{\sigma} \text{ is in MITE with respect to } \mathcal{A}_{\text{MITE}}^{(\text{few})} \iff \|\hat{\sigma} - \hat{\rho}_{\text{th}}\|_1^{(\mathcal{A}_{\text{MITE}}^{(\text{few})})} \leq \epsilon, \quad (\text{S10})$$

where $\epsilon \ll 1$.

C. Macroscopic thermal equilibrium (MATE) [1–3]

The notion of macroscopic thermal equilibrium (MATE) is introduced in Refs. [1, 2] as follows.

Definition II.2: Macroscopic thermal equilibrium (MATE) [2]

We consider a collection of macro observables $\hat{M}_1, \dots, \hat{M}_K$. By suitably coarse-graining the operators $\hat{M}_1, \dots, \hat{M}_K$, we expect to obtain a set of mutually commuting operators $\tilde{M}_1, \dots, \tilde{M}_K$ with $\tilde{M}_j \approx \hat{M}_j$ for all $j = 1, \dots, K$. We take \tilde{M}_1 as the coarse-grained Hamiltonian, whose eigenspaces are energy shells $\mathcal{H}_{E,\Delta E}$.

Since $\tilde{M}_1, \dots, \tilde{M}_K$ commute with each other, we can simultaneously diagonalize them, and the energy shell $\mathcal{H}_{E,\Delta E}$ can be decomposed accordingly as $\mathcal{H}_{E,\Delta E} = \bigoplus_{\nu} \mathcal{H}_{\nu}$. Here, \mathcal{H}_{ν} is called macro-spaces, and we denote the projector onto \mathcal{H}_{ν} by $\hat{\Pi}_{\nu}$.

In each $\mathcal{H}_{E,\Delta E}$, it is expected that one macro-space called thermal equilibrium macro-space \mathcal{H}_{eq} covers the most of the dimensions of $\mathcal{H}_{E,\Delta E}$, i.e.,

$$\frac{\dim \mathcal{H}_{\text{eq}}}{\dim \mathcal{H}_{E,\Delta E}} = 1 - \tilde{\epsilon}, \quad (\text{S11})$$

where $\tilde{\epsilon} \ll 1$. Without loss of generality, we set $\mathcal{H}_{\text{eq}} = \mathcal{H}_{\nu=1}$.

Under these setups, a state $\hat{\sigma} \in \dim \mathcal{H}_{E,\Delta E}$ is said to be in macroscopic thermal equilibrium (MATE) if and only if

$$\text{tr}(\hat{\sigma} \hat{\Pi}_{\text{eq}}) \geq 1 - \delta \quad (\text{S12})$$

for a sufficiently small tolerance $\delta > 0$.

As mentioned in Ref. [2], MATE can be regarded as the thermal equilibrium relative to the (coarse-grained) macroscopic observables $\tilde{M}_1, \dots, \tilde{M}_K$. Because we focus on the joint distribution of the observed values of $\tilde{M}_1, \dots, \tilde{M}_K$ in MATE, \mathcal{A} for MATE is given by

$$\mathcal{A}_{\text{MATE}} = \{\hat{\Pi}_{\text{eq}}\}. \quad (\text{S13})$$

Then, we have the following proposition.

Proposition II.3

Let $\hat{\sigma}$ be an arbitrary quantum state. Then,

$$\hat{\sigma} \text{ is in MATE with tolerance } \delta (\geq 2\tilde{\epsilon}). \iff \left\| \hat{\sigma} - \hat{\rho}_{\delta E}^{(\text{mc})} \right\|_1^{(\mathcal{A}_{\text{MATE}})} \leq \delta - \tilde{\epsilon}. \quad (\text{S14})$$

Proof. For $\mathcal{A}_{\text{MATE}} = \{\hat{\Pi}_{\text{eq}}\}$, we have

$$\left\| \hat{\sigma} - \hat{\rho}_{\delta E}^{(\text{mc})} \right\|_1^{(\mathcal{A}_{\text{MATE}})} = \left| \text{tr}(\hat{\sigma} \hat{\Pi}_{\text{eq}}) - \frac{\dim \mathcal{H}_{\text{eq}}}{\dim \mathcal{H}_{E, \Delta E}} \right|. \quad (\text{S15})$$

Therefore, $\left\| \hat{\sigma} - \hat{\rho}_{\delta E}^{(\text{mc})} \right\|_1^{(\mathcal{A}_{\text{MATE}})} \leq \epsilon$ is equivalent to

$$1 - (\tilde{\epsilon} + \epsilon) \leq \text{tr}(\hat{\sigma} \hat{\Pi}_{\text{eq}}) \leq 1 + (\epsilon - \tilde{\epsilon}). \quad (\text{S16})$$

By setting $\epsilon := \delta - \tilde{\epsilon}$ ($\geq \tilde{\epsilon}$), we obtain

$$\left\| \hat{\sigma} - \hat{\rho}_{\delta E}^{(\text{mc})} \right\|_1^{(\mathcal{A}_{\text{MATE}})} \leq \delta - \tilde{\epsilon} \iff 1 - \delta \leq \text{tr}(\hat{\sigma} \hat{\Pi}_{\text{eq}}), \quad (\text{S17})$$

which is the desired result. ■

Apart from quantum thermalization, the (semi-)norm $\|\cdot\|_1^{(\mathcal{A})}$ introduced in Eq. (1) in the main text serves as the measure of the closeness between two quantum states $\hat{\sigma}$ and $\hat{\rho}$ relative to \mathcal{A} . Thus, it can be used in various situations other than quantum thermal equilibrium and the ETH, such as a comparison between the state during time evolution and the steady state. In particular, it can be used to construct the space of macroscopic states from that of quantum states by identifying quantum states that are very close to each other in terms of $\|\cdot\|_1^{(\mathcal{A})}$. Rigorously formulating the correspondence between microscopic and macroscopic states in this direction and deriving the macroscopic dynamics from the microscopic one are important future problems.

III. LINEAR INDEPENDENCE OF BASIS OPERATORS FOR THE m -BODY OPERATOR SPACE

In this section, we show the linear independence of the basis operators

$$\hat{f}_{\mathbf{x}}^\dagger \hat{f}_{\mathbf{y}} := \hat{\Pi}_{N,V} \left(\hat{f}_{x_m}^\dagger \cdots \hat{f}_{x_1}^\dagger \hat{f}_{y_1} \cdots \hat{f}_{y_m} \right) \hat{\Pi}_{N,V}, \quad \begin{pmatrix} 1 \leq x_1 < \cdots < x_m \leq V \\ 1 \leq y_1 < \cdots < y_m \leq V \end{pmatrix} \quad (\text{S18})$$

of the fermionic m -body operator space, where $\mathbf{x} := \{x_1, \dots, x_m\}$ and $\mathbf{y} := \{y_1, \dots, y_m\}$. We decompose \mathbf{x} and \mathbf{y} as $\mathbf{x} = X \sqcup Z$ and $\mathbf{y} = Y \sqcup Z$, where “ \sqcup ” denotes the disjoint union, $Z := \mathbf{x} \cap \mathbf{y}$, $X := \mathbf{x} \setminus Z$, and $Y := \mathbf{y} \setminus Z$. Accordingly, we rearrange the product $\hat{f}_{y_1} \cdots \hat{f}_{y_m}$ by introducing

$$\hat{f}_{Y \sqcup Z} := \left(\prod_{x \in Y} \hat{f}_x \right) \left(\prod_{x \in Z} \hat{f}_x \right), \quad (\text{S19})$$

where the product \prod of the annihilation operators \hat{f}_x is arranged in the ascending order in x within each pair of parentheses.

To show the linear independence of the operators $\left\{ \hat{f}_{\mathbf{x}}^\dagger \hat{f}_{\mathbf{y}} \mid \begin{matrix} 1 \leq x_1 < \cdots < x_m \leq V, \\ 1 \leq y_1 < \cdots < y_m \leq V \end{matrix} \right\}$, we consider the equation

$$0 = \sum_{\substack{X,Y \\ X \cap Y = \emptyset \\ |X|=|Y| \leq \min\{m, V/2\}}} \sum_{\substack{Z \\ |Z|=m-|X| \\ Z \cap X = \emptyset, Z \cap Y = \emptyset}} C_{X,Y}(Z) (\hat{f}_{X \sqcup Z})^\dagger \hat{f}_{Y \sqcup Z} \quad (=:\hat{A}). \quad (\text{S20})$$

Given X and Y , we label the basis vectors of $\mathcal{H}_{N,V}$ as

$$|\mathbf{n}_X, \mathbf{n}_Y, \mathbf{n}_{\mathbf{V} \setminus (X \sqcup Y)}\rangle := \left(\prod_{x \in X} (\hat{f}_x)^{n_x} \right)^\dagger \left(\prod_{y \in Y} (\hat{f}_y)^{n_y} \right)^\dagger \left(\prod_{x \in \mathbf{V} \setminus (X \sqcup Y)} (\hat{f}_x)^{n_x} \right)^\dagger |0\rangle, \quad (\text{S21})$$

where $\mathbf{n}_W := \{n_x \in \{0, 1\} \mid x \in W\}$ with W being an arbitrary subset of $\mathbf{V} := \{1, \dots, V\}$. Then, taking the matrix element of the right-hand side of Eq. (S20), we obtain

$$\begin{aligned} & \langle \mathbf{n}_X = \mathbf{1}, \mathbf{n}_Y = \mathbf{0}, \mathbf{n}_{\mathbf{V} \setminus (X \sqcup Y)} | \hat{A} | \mathbf{n}_X = \mathbf{0}, \mathbf{n}_Y = \mathbf{1}, \mathbf{n}_{\mathbf{V} \setminus (X \sqcup Y)} \rangle \\ &= \sum_Z C_{X,Y}(Z) \langle \mathbf{n}_X = \mathbf{1}, \mathbf{n}_Y = \mathbf{0}, \mathbf{n}_{\mathbf{V} \setminus (X \sqcup Y)} | \hat{f}_{X \sqcup Z}^\dagger \hat{f}_{Y \sqcup Z} | \mathbf{n}_X = \mathbf{0}, \mathbf{n}_Y = \mathbf{1}, \mathbf{n}_{\mathbf{V} \setminus (X \sqcup Y)} \rangle \\ &= \sum_Z C_{X,Y}(Z) \langle \mathbf{n}_{\mathbf{V} \setminus (X \sqcup Y)} | \hat{f}_Z^\dagger \hat{f}_Z | \mathbf{n}_{\mathbf{V} \setminus (X \sqcup Y)} \rangle \\ &= \sum_Z C_{X,Y}(Z) \chi(\forall x \in Z, n_x = 1), \end{aligned} \quad (\text{S22})$$

where $\chi(\phi)$ is the indicator function that takes on unity if the proposition ϕ is true and zero otherwise. Therefore, the equation (S20) implies

$$\sum_{\substack{Z \\ |Z|=m-|X| \\ Z \cap X = \emptyset, Z \cap Y = \emptyset}} C_{X,Y}(Z) \chi(\forall x \in Z, n_x = 1) = 0 \quad (\text{S23})$$

for all X, Y , and $\mathbf{n}_{\mathbf{V} \setminus (X \cup Y)}$ with $|X| = |Y| \leq m$, $X \cap Y = \emptyset$, and $\sum_{x \in \mathbf{V} \setminus (X \cup Y)} n_x = N - |Y|$.

Here, the range of the summation over Z in Eq. (S23) depends only on X and Y and is independent of $\mathbf{n}_{\mathbf{V} \setminus (X \cup Y)}$, and the number of the summation over Z is given by

$$\binom{V - |X| - |Y|}{|Z|} = \binom{V - 2|X|}{m - |X|}. \quad (\text{S24})$$

On the other hand, the number of choices for $\mathbf{n}_{\mathbf{V} \setminus (X \cup Y)}$ in Eq. (S23) is

$$\binom{V - 2|X|}{N - |X|} \quad (\text{S25})$$

for given X and Y . When $N \leq V/2$, we have

$$m - |X| \leq N - |X| \leq \frac{V}{2} - |X| = \frac{V - 2|X|}{2}, \quad (\text{S26})$$

and therefore

$$\binom{V - 2|X|}{m - |X|} \leq \binom{V - 2|X|}{N - |X|} \quad (\text{S27})$$

for any $m \leq N$. This means that the number of equations (S23) for given X and Y is equal to or larger than the number of the coefficients $\{C_{X,Y}(Z)\}_Z$. Therefore, Eq. (S20) implies $C_{X,Y}(Z) = 0$ for all X, Y, Z when $N \leq V/2$. Thus, the linear independence of the operators $\{\hat{f}_{\mathbf{x}}^\dagger \hat{f}_{\mathbf{y}} \mid 1 \leq x_1 < \dots < x_m \leq V, 1 \leq y_1 < \dots < y_m \leq V\}$ is proved.

On the other hand, when $N > V/2$, we have

$$V - 2|X| - (N - |X|) = V - N - |X| \leq \frac{V - 2|X|}{2}. \quad (\text{S28})$$

Therefore, for $m > V - N$, the number of equations (S23) for given X and Y is less than the number of the coefficients $\{C_{X,Y}(Z)\}_Z$, and the operators in $\{\hat{f}_{\mathbf{x}}^\dagger \hat{f}_{\mathbf{y}} \mid 1 \leq x_1 < \dots < x_m \leq V, 1 \leq y_1 < \dots < y_m \leq V\}$ can be linearly dependent.

IV. NARROWING THE OPERATOR SPACE WHERE AN ETH-BREAKING OPERATOR TYPICALLY EXISTS FOR SYSTEMS WITH HAAR-DISTRIBUTED ENERGY EIGENSTATES

Theorem 2 in the main text shows that an ETH-breaking operator typically exists in $\mathcal{A}^{[0,\alpha V]}$ for any $\alpha > \alpha_U$. Here, we show that we can narrow such an operator space from $\mathcal{A}^{[0,\alpha V]}$ to $\mathcal{A}^{[m_{\bar{U}},m_{\bar{U}}^{\dagger}]}$, which is the orthogonal complement of $\mathcal{A}^{[0,m_{\bar{U}}^{\dagger}]}$ in $\mathcal{A}^{[0,m_{\bar{U}}^{-1}]}$ defined by

$$\mathcal{A}^{[m_{\bar{U}},m_{\bar{U}}^{\dagger}]} := \left\{ \hat{A} \in \mathcal{A}^{[0,m_{\bar{U}}^{\dagger}]} \mid \text{tr}[\hat{X}^{\dagger} \hat{A}] = 0, \forall \hat{X} \in \mathcal{A}^{[0,m_{\bar{U}}^{-1}]} \right\} \quad (\text{S29})$$

and

$$m_{\bar{U}} := N \max \left\{ \alpha_U - \frac{c_-}{\sqrt{N}}, 0 \right\}, \quad m_{\bar{U}}^{\dagger} := N \min \left\{ \alpha_U + \frac{c_+}{\sqrt{N}}, 1 \right\}, \quad (\text{S30})$$

where c_{\pm} are arbitrary positive constants independent of V . The dimension of the operator space $\mathcal{A}^{[m_{\bar{U}},m_{\bar{U}}^{\dagger}]}$ is given by $\dim \mathcal{A}^{[m_{\bar{U}},m_{\bar{U}}^{\dagger}]} = \dim \mathcal{A}^{[0,m_{\bar{U}}^{\dagger}]} - \dim \mathcal{A}^{[0,m_{\bar{U}}^{-1}]}$. The lower bound of Theorem 1 in the main text applied to $\mathcal{A}^{[m_{\bar{U}},m_{\bar{U}}^{\dagger}]}$ can be written as

$$\frac{\dim \mathcal{A}^{[m_{\bar{U}},m_{\bar{U}}^{\dagger}]} }{D^2} = \frac{\dim \mathcal{A}^{[0,m_{\bar{U}}^{\dagger}]} }{\dim \mathcal{A}^{[0,N]}} \left(1 - \frac{\dim \mathcal{A}^{[0,m_{\bar{U}}^{-1}]} }{\dim \mathcal{A}^{[0,m_{\bar{U}}^{\dagger}]} } \right), \quad (\text{S31})$$

where we use $\dim \mathcal{A}^{[0,N]} = D^2$ with D being the dimension of the Hilbert space.

Theorem IV.1

There exists an N -independent constant $\alpha_U > 0$ such that the ETH with respect to $\mathcal{A}^{[m_{\bar{U}},m_{\bar{U}}^{\dagger}]}$ typically breaks down in \mathcal{G}_{inv} . Here, $m_{\bar{U}}^{\pm}$ are defined in Eq. (S30).

Proof of Theorem IV.1 for spin systems. For spin systems, the dimension of the operator space $\mathcal{A}^{[m_{\bar{U}},m_{\bar{U}}^{\dagger}]}$ is given by

$$\dim \mathcal{A}^{[m_{\bar{U}},m_{\bar{U}}^{\dagger}]} = D^2 \sum_{j=m_{\bar{U}}^-}^{m_{\bar{U}}^{\dagger}} P_j, \quad (\text{S32})$$

where $D_N := \dim \mathcal{H}_N = (d_{\text{loc}})^N$ is the dimension of the N -spin Hilbert space \mathcal{H}_N , and $P_j := \binom{N}{j} \frac{(d_{\text{loc}}^2 - 1)^j}{d_{\text{loc}}^{2N}}$ with $d_{\text{loc}} := 2S + 1$ is the probability mass for the binomial distribution $\mathcal{B}(N, p)$ with $p = 1 - (d_{\text{loc}})^{-2}$. We use the fact that $\mathcal{B}(N, p)$ converges in distribution to a Gaussian distribution $\mathcal{N}(Np, Np(1-p))$ for large N . By setting $\alpha_U = p$, this fact implies that

$$\lim_{N \rightarrow \infty} \frac{\dim \mathcal{A}^{[m_{\bar{U}},m_{\bar{U}}^{\dagger}]} }{D^2} = \lim_{N \rightarrow \infty} \sum_{j=m_{\bar{U}}^-}^{m_{\bar{U}}^{\dagger}} P_j = \int_{-x_-}^{x_+} e^{-x^2/2} dx > 0, \quad (\text{S33})$$

where $x_{\pm} := c_{\pm}/\sqrt{p(1-p)}$. Then, Theorem 1 in the main text implies that the ETH with respect to $\mathcal{A}^{[m_{\bar{U}}, m_{\bar{U}}^{\dagger}]}$ typically breaks down in \mathcal{G}_{inv} for spin systems. ■

Proof of Theorem IV.1 for Bose systems. For Bose systems, Stirling's formula gives

$$\dim \mathcal{A}^{[0, m]} = \binom{V+m-1}{m}^2 = \exp \left[2V(1+n\alpha)H\left(\frac{1}{1+n\alpha}\right) - \log V + \mathcal{O}(1) \right], \quad (\text{S34})$$

where $n := N/V$, $\alpha := m/V$, and $H(x) := -x \log x - (1-x) \log(1-x)$. Since the function $xH(1/x)$ is a monotonically increasing function of x , the first factor ($\dim \mathcal{A}^{[0, m_{\bar{U}}^{\dagger}]}/\dim \mathcal{A}^{[0, N]}$) in Eq. (S31) converges to a positive value only if $\lim_{N \rightarrow \infty} (m_{\bar{U}}^{\dagger}/N) = 1$. Therefore, we must set $\alpha_{\bar{U}} = 1$ for Bose systems. The second factor $1 - \dim \mathcal{A}^{[0, m_{\bar{U}}^{-1}]} / \dim \mathcal{A}^{[0, m_{\bar{U}}^{\dagger}]}$ remains finite because $m_{\bar{U}}^{-1} \leq m_{\bar{U}}^{\dagger}$ by definition. This can be seen as

$$1 - \frac{\dim \mathcal{A}^{[0, m_{\bar{U}}^{-1}]}}{\dim \mathcal{A}^{[0, m_{\bar{U}}^{\dagger}]}} \geq 1 - \frac{\dim \mathcal{A}^{[0, m_{\bar{U}}^{\dagger}-1]}}{\dim \mathcal{A}^{[0, m_{\bar{U}}^{\dagger}]}} = 1 - \left(\frac{m_{\bar{U}}^{\dagger}}{V + m_{\bar{U}}^{\dagger} - 1} \right)^2 \xrightarrow{N \rightarrow \infty} \frac{1 + 2n}{(1+n)^2} > 0. \quad (\text{S35})$$

These facts show that the left-hand side of Eq. (S31) remains finite. Thus, the proof of Theorem IV.1 for Bose systems is completed. ■

Proof of Theorem IV.1 for Fermi systems. For (spinless) Fermi systems, Stirling's formula gives

$$\dim \mathcal{A}^{[0, m]} = \binom{V}{\min\{m, V-N\}}^2 = \begin{cases} \exp[2VH(n\alpha) - \log V + \mathcal{O}(1)] & (\alpha \leq \frac{1-n}{n}); \\ \dim \mathcal{A}^{[0, N]} & (\alpha \geq \frac{1-n}{n}), \end{cases} \quad (\text{S36})$$

where $n := N/V$, $\alpha := m/V$, and $H(x) := -x \log x - (1-x) \log(1-x)$.

Here, the function $H(n\alpha)$ is a monotonically increasing function of α in the region $n\alpha \in [0, \min\{1-n, n\}] \subset [0, 1/2]$. Thus, the first factor ($\dim \mathcal{A}^{[0, m_{\bar{U}}^{\dagger}]}/\dim \mathcal{A}^{[0, N]}$) in Eq. (S31) converges to a positive value only if $\alpha_{\bar{U}} = \lim_{N \rightarrow \infty} (m_{\bar{U}}^{\dagger}/N) \geq \min\{(1-n)/n, 1\}$.

In addition, the second factor $1 - \dim \mathcal{A}^{[0, m_{\bar{U}}^{-1}]} / \dim \mathcal{A}^{[0, m_{\bar{U}}^{\dagger}]}$ remains finite only when $\alpha_{\bar{U}} = \lim_{N \rightarrow \infty} (m_{\bar{U}}^{-1}/N) \leq \min\{(1-n)/n, 1\}$. This can be seen as

$$1 - \frac{\dim \mathcal{A}^{[0, m_{\bar{U}}^{-1}]}}{\dim \mathcal{A}^{[0, m_{\bar{U}}^{\dagger}]}} \geq 1 - \frac{\dim \mathcal{A}^{[0, m_{\bar{U}}^{-1}]}}{\dim \mathcal{A}^{[0, m_{\bar{U}}^{-1}]}} \xrightarrow{N \rightarrow \infty} 1 - \left(\frac{n\alpha_{\bar{U}}}{1-n\alpha_{\bar{U}}} \right)^2. \quad (\text{S37})$$

The right-most-hand side becomes finite when $n\alpha_{\bar{U}} < 1/2$, which is satisfied because of $\alpha_{\bar{U}} \leq \min\{(1-n)/n, 1\}$. These facts show that the left-hand side of Eq. (S31) remains finite if we set $\alpha_{\bar{U}} = \{(1-n)/n, 1\}$. Thus, the proof of Theorem IV.1 for Fermi systems is completed. ■

V. DETAILS ON THE NUMERICAL CALCULATIONS

To numerically test our Conjecture 1 for systems with local and few-body interactions introduced in the Methods section of the main text, we calculate the quantity

$$\Lambda_2^{(\hat{H}, \mathcal{A}^{[0,m]})} := \max_{|E_\alpha\rangle, |E_\beta\rangle \in \mathcal{H}_{E_x, \Delta}} \left\| |E_\alpha\rangle\langle E_\beta| - \delta_{\alpha\beta} \hat{\rho}_{\delta E}^{(\text{mc})}(E_\alpha) \right\|_2^{(\mathcal{A}^{[0,m]})}, \quad (\text{S38})$$

where $\mathcal{A}^{[0,m]}$ is the m -body operator space, $|E_\alpha\rangle$ is an eigenstate of \hat{H} such that $\hat{H}|E_\alpha\rangle = E_\alpha|E_\alpha\rangle$, $\mathcal{H}_{E, \kappa} := \text{span}\{|E_\gamma\rangle \mid |E_\gamma - E| \leq \kappa\}$ is an energy shell centered at energy E with width 2κ , $\hat{\rho}_{\delta E}^{(\text{mc})}(E_\alpha)$ is the microcanonical density operator on the shell $\mathcal{H}_{E_\alpha, \delta E}$. Here, the center E_x and the width Δ of the region for the test of the ETH are chosen to be $E_x := xE_{\text{max}} + (1-x)E_{\text{min}}$ and $\Delta := 0.025(E_{\text{max}} - E_{\text{min}})$, where $E_{\text{max}}/_{\text{min}}$ is the maximum/minimum eigenvalue of \hat{H} . Since the spectral width $(E_{\text{max}} - E_{\text{min}})$ is an extensive quantity for locally interacting systems [4], the normalized $x = (E - E_{\text{min}})/(E_{\text{max}} - E_{\text{min}})$ essentially serves as an energy density. The width of the microcanonical energy shell is set to be $\delta E = 0.2(E_{\text{max}} - E_{\text{min}})/V$, which is sufficiently small to exclude contributions from the energy dependence of the microcanonical average within the shell $\mathcal{H}_{E_\alpha, \delta E}$ for the system sizes of our numerical calculations (up to 18 spins for spin systems, and up to 11 particles for boson systems at unit filling and fermion systems at half filling).

The quantity $\Lambda_2^{(\hat{H}, \mathcal{A}^{[0,m]})}$ can be calculated by computing the 2-norm on the right-hand side of Eq. (S38) for all $|E_\alpha\rangle, |E_\beta\rangle \in \mathcal{H}_{E_x, \Delta}$. This can be done by using the explicit formula (4) in the Methods section of the main text. The calculation of the 2-norm requires $\mathcal{O}(MD)$ steps for each $(\alpha\beta)$, where $M := \dim(\mathcal{A}^{[0,m]} + \mathbb{R}\hat{I})$ and $D := \dim \mathcal{H}$. Thus, the computation of $\Lambda_2^{(\hat{H}, \mathcal{A}^{[0,m]})}$ requires $\mathcal{O}(MD^3)$ steps. This computational cost is much heavier than the cost $\mathcal{O}(D^3)$ of numerical diagonalization of \hat{H} . Therefore, we restrict ourselves to the numerical verification of the diagonal part of the ETH, for which we calculate

$$\tilde{\Lambda}_2^{[0,m]} := \tilde{\Lambda}_2^{(\hat{H}, \mathcal{A}^{[0,m]})} := \max_{|E_\alpha\rangle \in \mathcal{H}_{E_x, \Delta}} \left\| |E_\alpha\rangle\langle E_\alpha| - \hat{\rho}_{\delta E}^{(\text{mc})}(E_\alpha) \right\|_2^{(\mathcal{A}^{[0,m]})}. \quad (\text{S39})$$

It bounds the restriction of the m -body ETH measure $\Lambda_1^{(\hat{H}, \mathcal{A}^{[0,m]})}$ to the diagonal ETH, which we denote $\tilde{\Lambda}_1^{(\hat{H}, \mathcal{A}^{[0,m]})}$, as $\tilde{\Lambda}_2^{(\hat{H}, \mathcal{A}^{[0,m]})} \leq \tilde{\Lambda}_1^{(\hat{H}, \mathcal{A}^{[0,m]})} \leq \sqrt{D} \tilde{\Lambda}_2^{(\hat{H}, \mathcal{A}^{[0,m]})}$. For notational simplicity, we rewrite $\tilde{\Lambda}_2^{[0,m]}$ as $\Lambda_2^{[0,m]}$ in the following.

To use the formula (4) in the Methods section of the main text, we need an orthonormal basis $\{\hat{\Lambda}_\mu\}_{\mu=1}^M$ of the operator space $\mathcal{A}^{[0,m]} + \mathbb{R}\hat{I}$. For spin-1/2 systems, it is given by

$$\{\hat{\Lambda}_\mu\} = \{2^{-V/2}\hat{I}\} \sqcup \left\{ 2^{-V/2} \hat{\sigma}_{x_1}^{(p_1)} \dots \hat{\sigma}_{x_m}^{(p_m)} \mid \substack{1 \leq x_1 < x_2 < \dots < x_m \leq V \\ \forall p_j \in \{1, 2, 3\} \ (j=1, \dots, m)} \right\}. \quad (\text{S40})$$

For boson and fermion systems, the naive basis operators $\{\hat{\alpha}(\mathbf{x}, \mathbf{y}) := \hat{a}_{x_1}^\dagger \cdots \hat{a}_{x_m}^\dagger \hat{a}_{y_1} \cdots \hat{a}_{y_m}\}$ are not orthogonal to one another, where \hat{a} is a bosonic or fermionic annihilation operator, and we introduce $\mathbf{x} = (x_1, \dots, x_m)$ and $\mathbf{y} = (y_1, \dots, y_m)$. An orthonormal basis can be obtained from the Gram matrix $G_{(\mathbf{x}, \mathbf{y}), (\mathbf{x}', \mathbf{y}')} := \text{tr}_N[\hat{\alpha}(\mathbf{x}, \mathbf{y})^\dagger \hat{\alpha}(\mathbf{x}', \mathbf{y}')] as$

$$\left\{ \hat{\Lambda}_\mu := \sum_{(\mathbf{x}, \mathbf{y})} \hat{\alpha}(\mathbf{x}, \mathbf{y}) (G^{-1/2})_{(\mathbf{x}, \mathbf{y}), \mu} \right\}_{\mu=1}^M. \quad (\text{S41})$$

Here, tr_N denotes the trace over the N -particle Hilbert space \mathcal{H}_N . For Hermitian operator \hat{X} , substituting this orthonormal basis into the formula (4) in the Methods section of the main text, we obtain

$$\begin{aligned} \|\hat{X}\|_2^{(\mathcal{A})} &= \|\vec{X}\|_2^2 = \sqrt{\sum_{\mu=1}^M \left| \sum_{(\mathbf{x}, \mathbf{y})} \text{tr}[\hat{\alpha}(\mathbf{x}, \mathbf{y})^\dagger \hat{X}] (G^{-1/2})_{(\mathbf{x}, \mathbf{y}), \mu}^* \right|^2} \\ &= \sqrt{\sum_{(\mathbf{x}, \mathbf{y})} \sum_{(\mathbf{x}', \mathbf{y}')} \text{tr}[\hat{\alpha}(\mathbf{x}, \mathbf{y})^\dagger \hat{X}]^* \left(\sum_{\mu=1}^M (G^{-1/2})_{(\mathbf{x}, \mathbf{y}), \mu} (G^{-1/2})_{(\mathbf{x}', \mathbf{y}'), \mu}^* \right) \text{tr}[\hat{\alpha}(\mathbf{x}', \mathbf{y}')^\dagger \hat{X}]} \\ &= \sqrt{\sum_{(\mathbf{x}, \mathbf{y})} \sum_{(\mathbf{x}', \mathbf{y}')} \text{tr}[\hat{\alpha}(\mathbf{x}, \mathbf{y})^\dagger \hat{X}]^* (G^{-1})_{(\mathbf{x}, \mathbf{y}), (\mathbf{x}', \mathbf{y}')} \text{tr}[\hat{\alpha}(\mathbf{x}', \mathbf{y}')^\dagger \hat{X}]} \end{aligned} \quad (\text{S42})$$

We use this formula to calculate the 2-norm given the Gram matrix G and the inner products $\{\text{tr}[\hat{\alpha}(\mathbf{x}, \mathbf{y})^\dagger \hat{X}]\}$. In general, the calculation of the formula (S42) requires $\mathcal{O}(DM^2)$ steps for the calculation of the Gram matrix and $\mathcal{O}(M^3)$ steps for calculating $\sum_{(\mathbf{x}', \mathbf{y}')} (G^{-1})_{(\mathbf{x}, \mathbf{y}), (\mathbf{x}', \mathbf{y}')} \text{tr}[\hat{\alpha}(\mathbf{x}', \mathbf{y}')^\dagger \hat{X}]$. These costs are too heavy compared with the diagonalization cost $\mathcal{O}(D^3)$ since M can be much larger than D . However, we find that the Gram matrix G has a block-diagonal structure, and the size of each block is reasonably small. Moreover, for \hat{X} that is invariant under the shift operations, i.e., $\hat{T} \hat{X} \hat{T}^\dagger = \hat{X}$ with $\hat{T} \hat{a}_j \hat{T}^\dagger := \hat{a}_{j+1}$, these blocks can be classified to orbits under the action of \hat{T} . Since the blocks belonging to the same orbit give the same contribution to $\|\hat{X}\|_2^{(\mathcal{A})}$, we can further reduce the number of blocks we need to compute.

The block-diagonal structure of the Gram matrix can be found as follows. In order to have a nonzero value of the inner product $\text{tr}_N[\hat{\alpha}(\mathbf{x}, \mathbf{y})^\dagger \hat{\alpha}(\mathbf{x}', \mathbf{y}')] as$, we must have $\hat{\alpha}(\mathbf{x}, \mathbf{y}) |\mathbf{n}\rangle = C_{\mathbf{n}} \hat{\alpha}(\mathbf{x}', \mathbf{y}') |\mathbf{n}\rangle$ ($C_{\mathbf{n}} \neq 0$) for some basis vector $|\mathbf{n}\rangle := \hat{a}_{n_1}^\dagger \cdots \hat{a}_{n_N}^\dagger |0\rangle$. By introducing the multisets $\mathcal{X} := \{x_j\}_{j=1}^m$, $\mathcal{Y} := \{y_j\}_{j=1}^m$, $\mathcal{X}' := \{x'_j\}_{j=1}^m$, and $\mathcal{Y}' := \{y'_j\}_{j=1}^m$, this condition is satisfied only when $\mathcal{X} \setminus \mathcal{Y} = \mathcal{X}' \setminus \mathcal{Y}'$ and $\mathcal{Y} \setminus \mathcal{X} = \mathcal{Y}' \setminus \mathcal{X}'$, which give rise to the block-diagonal structure of the Gram matrix. For example, the Gram matrix for boson systems with $V = N = 10$ and $m = 4$ are

found to consist of the following blocks:

Block size	# of blocks of the same size	# of orbits by the shift operation
715	1	1
220	90	9
55	2070	209
10	22530	2253
1	151560	15167

(S43)

Given that $M = 511225$ in this case, we can drastically reduce the numerical costs in calculating the 2-norm by exploiting the block-diagonal structure of the Gram matrix, enabling numerical tests of Conjecture 1 for boson and (spinless) fermion systems up to $N = 11$ particles.

VI. ENERGY DEPENDENCE OF THE BOUNDS ON THE RATIO m_*/N

Figure 2 in the main text shows the numerical results for the upper bound $\sqrt{D}\Lambda_2^{[0,m]}$ of the diagonal ETH measure at the center of the energy spectrum ($E_x = E_{0.5} = (E_{\max} + E_{\min})/2$), where $\Lambda_2^{[0,m]}$ is given in Eq. (S39). Here, we present numerical results for locally interacting systems at varying normalized energies $x = (E - E_{\min})/(E_{\max} - E_{\min})$ in Figs. S1-S3.

As in the case for Fig. 2 in the main text, when x is not small, we can find the point $\alpha_L(x)$ where the curves of the upper bound $\sqrt{D}\Lambda_2^{[0,m]}$ on the ETH measure for different system sizes intersect almost at a single point (Figs. S2 and Figs. S3). This intersection point decreases as the normalized energy deviates from the center $x = 0.5$, as shown in Fig. S1. For small values of $x \lesssim 0.25$, the intersection is no longer observed, suggesting the possibility that $m_*/N \rightarrow 0$ as $N \rightarrow \infty$ in this energy region. For spin systems, the intersection point $\alpha_U(x)$ for the lower bound $\Lambda_2^{[0,m]}$ of the diagonal ETH measure is also observed. This intersection point decreases as the normalized energy decreases, as in the case for $\alpha_L(x)$ (Fig. S1). These intersection points $\alpha_L(x)$ and $\alpha_U(x)$ are numerically calculated as the points where the maximum difference between the curves of $\mathbb{E}_{\log}(\sqrt{D}\Lambda_2^{[0,m]})^2$ and $\mathbb{E}_{\log}(\Lambda_2^{[0,m]})^2$ for different system sizes, as shown in Figs. S2 and S3, becomes minimum. Here, for a positive random variable X , $\mathbb{E}_{\log}[X]$ denotes the geometric mean given by $\mathbb{E}_{\log}[X] = \exp\left[\frac{1}{k} \sum_{j=1}^k \log X_k\right]$.

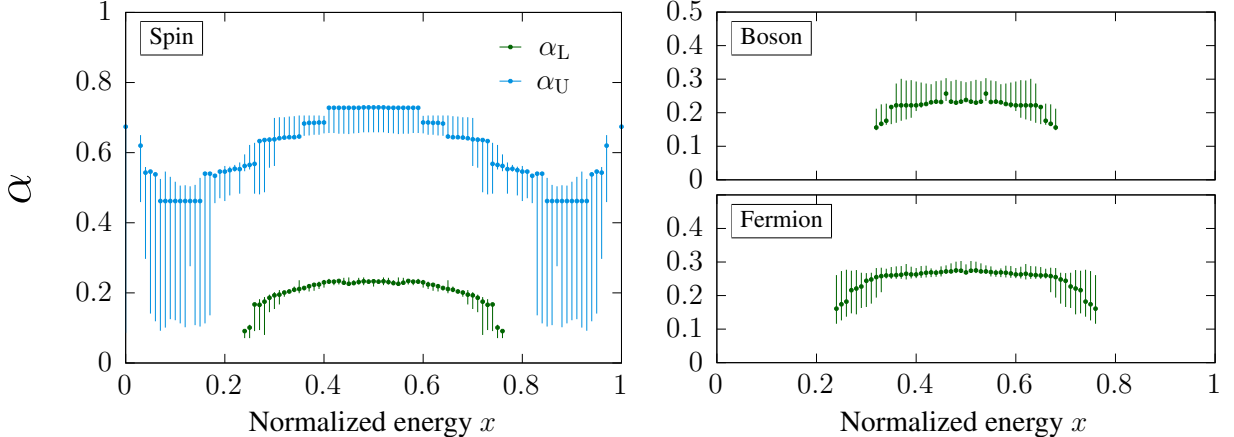


FIG. S1. **Energy dependence of the bounds α_L and α_U on the ratio m_*/N .** The data points indicate the value of m/N where the maximum difference between the curves with different system sizes for a fixed normalized energy in Figs. S2 and S3 becomes minimal. The upper/lower end of the error bars shows the value of m/N above which $\mathbb{E}_{\log}(\sqrt{D}\Lambda_2^{[0,m]})^2$ (or $\mathbb{E}_{\log}(\Lambda_2^{[0,m]})^2$) monotonically increases/decreases as the system size increases. The system sizes used in this figure are $14 (11) \leq N \leq 18 (14)$ for α_L (α_U) of spin systems and $8 \leq N \leq 11$ for Bose and Fermi systems.

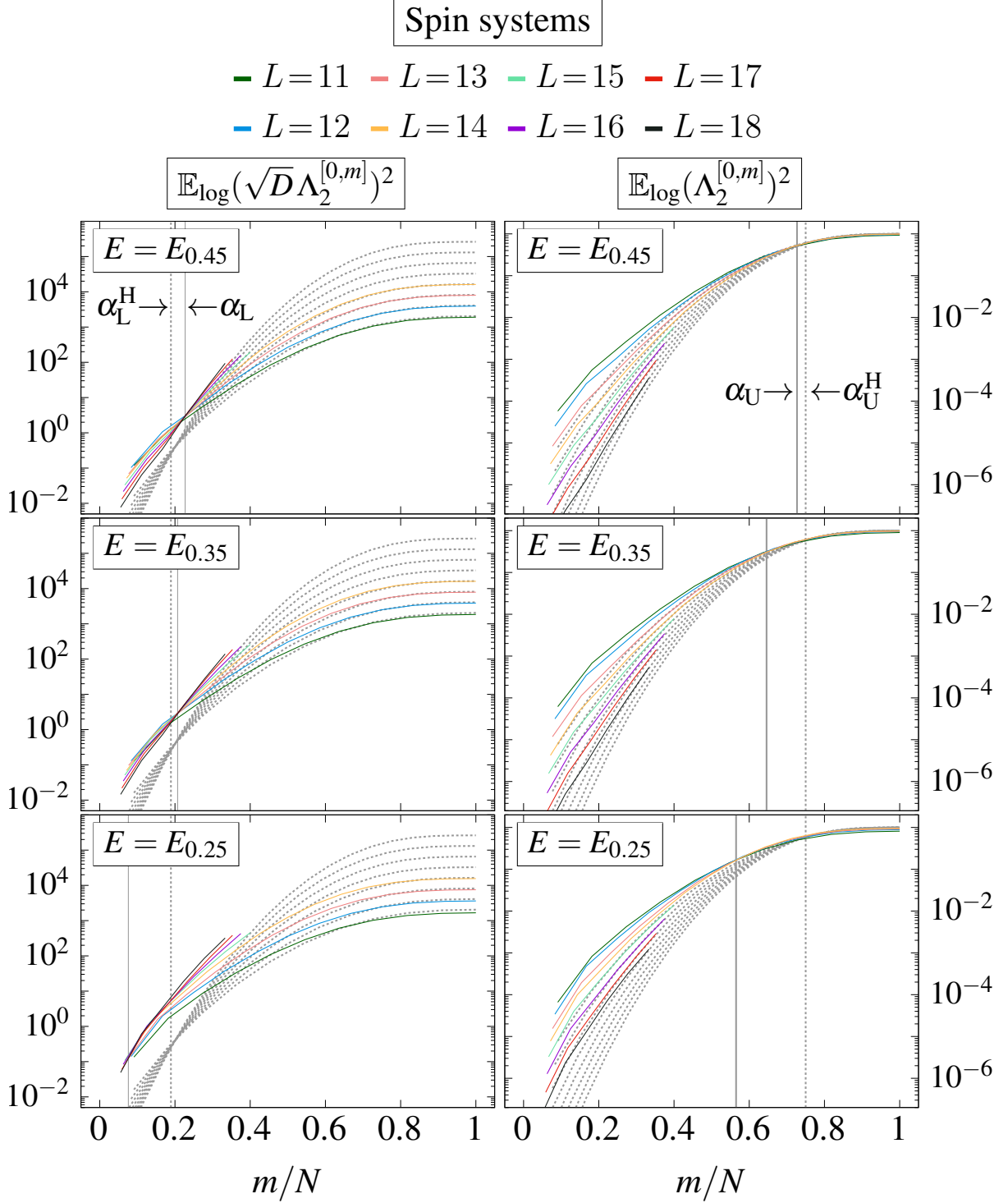


FIG. S2. Upper and lower bounds on the (diagonal) ETH measure for varying the normalized energy in locally interacting spin systems. The intersection point $\alpha_L(x)$ of $\mathbb{E}_{\log}(\sqrt{D}\Lambda_2^{[0,m]})^2$ is observed for non-small x but not observed for small $x \lesssim 0.25$. The intersection point $\alpha_U(x)$ of $\mathbb{E}_{\log}(\Lambda_2^{[0,m]})^2$ is also observed for all values of x . The intersection points for systems with Haar-distributed energy eigenstates are denoted by α_L^H and α_U^H .

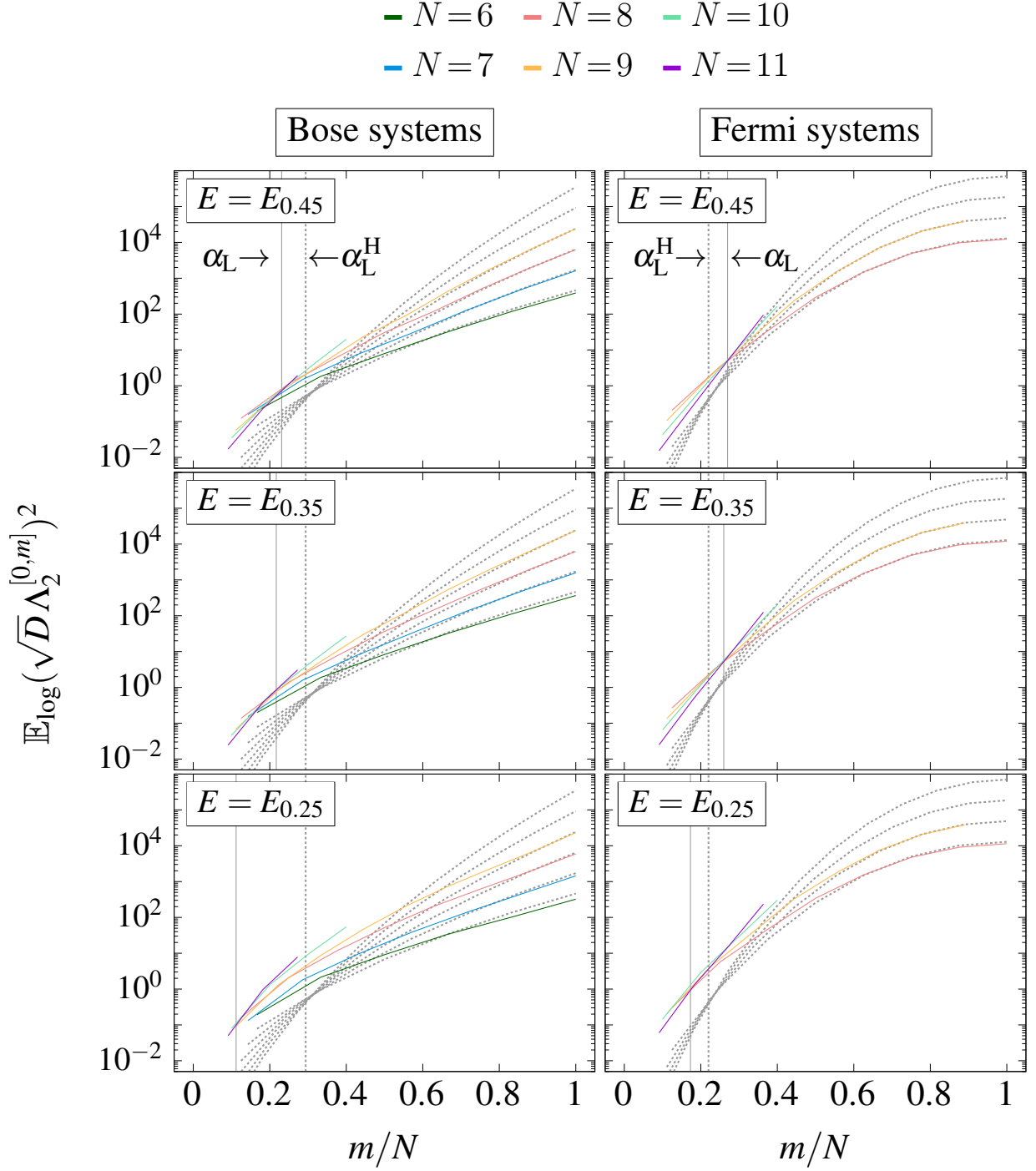


FIG. S3. Upper bound on the (diagonal) ETH measure for varying the normalized energy in locally interacting Bose and Fermi systems. The intersection point $\alpha_L(x)$ of $\mathbb{E}_{\log}(\sqrt{D}\Lambda_2^{[0,m]})^2$ can be observed for Fermi systems at non-small x . While it is less clear for Bose systems, the intersections still occur in a narrow region around the vertical solid lines for non-small x . The intersection is not observed for small x ($\lesssim 0.25$) within the system sizes of the numerical calculation (up to $N = 11$). The intersection point for systems with Haar-distributed energy eigenstates is denoted by α_L^H .

VII. NUMERICAL RESULTS FOR CONCRETE PHYSICAL MODELS

In this section, we show the numerical results for the following prototypical models of nonintegrable systems:

- Spin: We consider the mixed-field Ising model, whose Hamiltonian is given by

$$\hat{H} = J_x \sum_{j=1}^L \hat{\sigma}_j^{(x)} \hat{\sigma}_{j+1}^{(x)} + B_z \sum_{j=1}^L \hat{\sigma}_j^{(z)} + B_x \sum_{j=1}^L \hat{\sigma}_j^{(x)}, \quad (\text{S44})$$

where $\hat{\sigma}_j^{(p)}$ ($p \in \{x, y, z\}$) is a Pauli operator acting on site j . This model is numerically verified to satisfy the ETH in Ref. [5] for the parameter $(J_x, B_z, B_x) = (1, 0.9045, 0.8090)$.

- Boson: We consider the Bose-Hubbard model, whose Hamiltonian is given by

$$\hat{H} = -J \sum_{x=1}^L (\hat{b}_x^\dagger \hat{b}_{x+1} + \hat{b}_{x+1}^\dagger \hat{b}_x) - U \sum_{x=1}^L \frac{\hat{n}_x(\hat{n}_x - 1)}{2}. \quad (\text{S45})$$

This model at unit filling ($N/V = 1$) is numerically verified to satisfy the ETH in Ref. [6] for the parameter $(J, U) = (1, 1)$, where it is known to be nonintegrable [7]. We use these parameters in the numerical calculations.

- Fermion: We consider the spinless fermions with next-nearest hopping and interactions:

$$\begin{aligned} \hat{H} = & -t_1 \sum_{x=1}^L (\hat{f}_x^\dagger \hat{f}_{x+1} + \hat{f}_{x+1}^\dagger \hat{f}_x) - J_1 \sum_{x=1}^L \hat{n}_x \hat{n}_{x+1} \\ & - t_2 \sum_{x=1}^L (\hat{f}_x^\dagger \hat{f}_{x+2} + \hat{f}_{x+2}^\dagger \hat{f}_x) - J_1 \sum_{x=1}^L \hat{n}_x \hat{n}_{x+2}. \end{aligned} \quad (\text{S46})$$

This model is numerically verified to exhibit quantum chaotic behavior in Ref. [8] for $(t_1, J_1, t_2, J_2) = (1, 1, 0.32, 0.32)$ and $N/V = 1/3$. In our numerical calculation, we use these values of (t_1, J_1, t_2, J_2) but set $N/V = 1/2$.

We adopt periodic boundary conditions in all the models listed above. Since these systems have translation and reflection symmetries, we focus on the zero-momentum and even-parity sector.

Figure S4 shows the upper bound $\sqrt{D}\Lambda_2^{[0,m]}$ on the (diagonal) ETH measure at the center of the energy spectrum as a function of m/N . We observe that some of the curves with different system sizes intersect with each other. However, unlike the case for generic locally interacting systems in Figs. S2 and S3, the point where curves for various system sizes almost intersect is not observed for the nonintegrable models in Eqs. (S44)-(S46). Thus, it remains to be an open question whether the ratio m_*/N converges to a finite value or vanishes in the thermodynamic limit for these models.

It is interesting that the finite-size behaviors of $\sqrt{D}\Lambda_2^{[0,m]}$ are different in the nonintegrable models and the generic locally interacting systems presented in the methods section of the main text, even though these systems share the essential physical structure of the locality and the few-body nature of interactions. Investigating the underlying causes of these differences will be an important future problem.

Figure S5 shows the same data as in Fig. S4 as a function of the system size. For the mixed-field Ising model (S44) and the spinless fermion model (S46), the upper bound $\sqrt{D}\Lambda_2^{[0,m]}$ with $m \in [1, 4]$ decreases for the three largest system sizes. However, the number of these data points is too small, and the V -dependence of $\sqrt{D}\Lambda_2^{[0,m]}$ is not smooth for the system sizes of the numerical calculation. For the Bose-Hubbard model (S45), the upper bound $\sqrt{D}\Lambda_2^{[0,m]}$ with $m = 1$ almost monotonically decreases for $V \geq 6$. However, the curves for $m = 2, 3$ increase as V increases from 10 to 11, which are the two largest system sizes in our calculation. These facts indicate that the finite-size effects are nonnegligible in determining the behavior of $\sqrt{D}\Lambda_2^{[0,m]}$ for large V in the nonintegrable models in Eqs. (S44)-(S46).

The large finite-size effects of $\sqrt{D}\Lambda_2^{[0,m]}$ in Figs. S4 and S5 may suggest that the inequality $\|\cdot\|_1^{(\mathcal{A})} \leq \sqrt{D}\|\cdot\|_2^{(\mathcal{A})}$ is too loose to test Conjecture 1 in the main text for those concrete physical models. It remains to be an important future task to validate (or invalidate) Conjecture 1 for prototypical nonintegrable systems, e.g., by finding better bounds on the ETH measure. The inequality $\|\cdot\|_2^{(\mathcal{A})} \leq \|\cdot\|_1^{(\mathcal{A})}$ may also be too loose because it fails to provide $\alpha_U < 0.5$ for spin and Bose systems with Haar-distributed energy eigenstates. For Fermi systems with Haar-distributed energy eigenstates, it gives a better estimate on α_U in the high-density region ($n := N/V > 2/3$) as $\alpha_U = (1 - n)/n < 1/2$, but does not in the other region with $n < 2/3$. The bound $\alpha_U < 0.5$ is expected from a probable argument based on the comparison of the reduced density operators of energy eigenstates and a thermal ensemble on a subsystem [9]. Therefore, it remains to be a future problem to improve the value of α_U by, for example, finding a better lower bound on $\|\cdot\|_1^{(\mathcal{A})}$ or quantifying quantum correlations associated with the decomposition of the operator space into accessible part \mathcal{A} and inaccessible part.

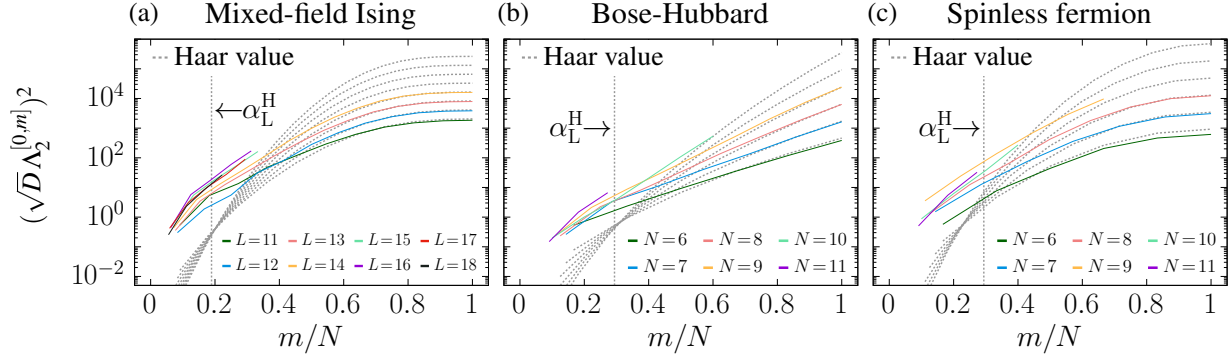


FIG. S4. Upper bound on the (diagonal) ETH measure as a function of m/N for the non-integrable models in Eqs. (S44)-(S46). The upper bounds are calculated at the center of the energy spectrum. While some of the curves intersect with each other, they do not intersect at a single point within the system sizes of the numerical calculation.

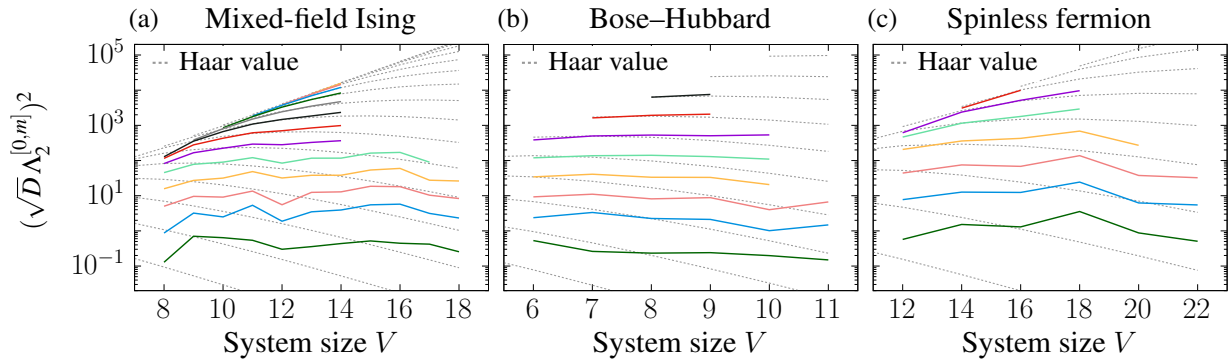


FIG. S5. Upper bound on the (diagonal) ETH measure as a function of V for the nonintegrable models in Eqs. (S44)-(S46). The same data as in Fig. S4 are shown as a function of the system size. Different colors indicate different values of m ranging from 1 to N . The upper bound $\sqrt{D}\Lambda_2^{[0,m]}$ with $m \in [1, 4]$ decreases as V increases in the region $V \geq 16$ for the spin system and $V \geq 9$ for the spinless fermions. However, the number of data points in these regions is too small, and the V -dependence of $\sqrt{D}\Lambda_2^{[0,m]}$ is not smooth. For the boson system, the upper bound $\sqrt{D}\Lambda_2^{[0,m]}$ with $m = 1$ smoothly decreases for $V \geq 6$. However, the curves for $m = 2, 3$ increase as V increases from 10 to 11, which are the two largest system sizes in our calculation. These facts indicate that the finite-size effects are nonnegligible in determining the behavior of $\sqrt{D}\Lambda_2^{[0,m]}$ for large V in the nonintegrable models in Eqs. (S44)-(S46).

-
- [1] S. Goldstein, D. A. Huse, J. L. Lebowitz, and R. Tumulka, Thermal Equilibrium of a Macroscopic Quantum System in a Pure State, [Physical Review Letters](#) **115**, 100402 (2015).
 - [2] S. Goldstein, D. A. Huse, J. L. Lebowitz, and R. Tumulka, Macroscopic and microscopic thermal equilibrium, [Annalen der Physik](#) **529**, 1600301 (2017).
 - [3] T. Mori, T. N. Ikeda, E. Kaminishi, and M. Ueda, Thermalization and prethermalization in isolated quantum systems: a theoretical overview, [Journal of Physics B: Atomic, Molecular and Optical Physics](#) **51**, 112001 (2018).
 - [4] H. Tasaki, On the Local Equivalence Between the Canonical and the Microcanonical Ensembles for Quantum Spin Systems, [Journal of statistical physics](#) **172**, 905 (2018).
 - [5] H. Kim, T. N. Ikeda, and D. A. Huse, Testing whether all eigenstates obey the eigenstate thermalization hypothesis, [Physical Review E](#) **90**, 052105 (2014).
 - [6] G. Biroli, C. Kollath, and A. M. Läuchli, Effect of Rare Fluctuations on the Thermalization of Isolated Quantum Systems, [Physical Review Letters](#) **105**, 250401 (2010).
 - [7] A. R. Kolovsky and A. Buchleitner, Quantum chaos in the Bose-Hubbard model, [Europhysics letters](#) **68**, 632 (2004).
 - [8] L. F. Santos and M. Rigol, Onset of quantum chaos in one-dimensional bosonic and fermionic systems and its relation to thermalization, [Physical Review E](#) **81**, 036206 (2010).
 - [9] J. R. Garrison and T. Grover, Does a Single Eigenstate Encode the Full Hamiltonian?, [Physical Review X](#) **8**, 021026 (2018)